Electronic Supplementary Material (ESI) for Dalton Transactions.
This journal is © The Royal Society of Chemistry 2023

Electronic supplementary information for:

Mitochondria-Targeted Neutral and Cationic Iridium(III) Anticancer Complexes Chelating Simple Hybrid sp^2-N/sp^3-N Donor Ligands

in Honor of Professor Thomas R. Ward on His 60th Birthday

Pengwei Li, Lihua Guo*, Jiaxing Li, Zhihao Yang, Hanxiu Fu, Kangning Lai, Heqian Dong, Chunyan Fan, Zhe Liu*

Key Laboratory of Life-Organic Analysis of Shandong Province, Key Laboratory of Green Natural Products and Pharmaceutical Intermediates in Colleges and Universities of Shandong Province, Institute of Anticancer Agents Development and Theranostic Application, School of Chemistry and Chemical Engineering, Qufu Normal University, Qufu 273165, P. R. China

*Corresponding Author: Email: guolihua@qfnu.edu.cn (L. H. Guo); liuzheqd@163.com (Z. Liu).

1.EXPERIMENTAL SECTIONS

1.1. Solution Stability Studies.

Solution of complexes **Ir1**-**Ir12** with final concentration of 50 μM in 10% DMSO/90% PBS (pH ≈ 7.4, PBS is prepared from H_2O), were prepared by dissolution of the complexes in DMSO followed by rapid dilution with PBS. UV-vis spectra of the solution were recorded at 37 °C after various time intervals. Solutions of complexes **Ir1**, **Ir8** and **Ir9** final concentration of 0.5 mM in 75% DMSO-d_6/25% phosphate-buffered saline (PBS) (pH ≈ 7.4, PBS is prepared from D_2O) was monitored by ^{1}H NMR. ^{1}H NMR spectra were recorded after various time intervals at 37 °C.

1.2. Cell Culture Conditions.

Human cells (A549 cells, A549/DDP cells, HeLa cells, HepG2 cells and BESA-2B cells) were obtained from Shanghai Institute of Biochemistry. The cells were maintained in DMEM (Dulbecco's modified Eagle's medium, Gibco BRL) or RPMI 1640 (Roswell Park Memorial Institute 1640, Gibco BRL) medium, which contained 10% FBS (fetal bovine serum, Gibco BRL), 100 μg mL^{-1} streptomycin, and 100 U mL^{-1} penicillin (Gibco BRL). The cells were cultured in a humidified incubator, which provided an atmosphere of 5% CO_2 and 95% air at a constant temperature of 37 °C.

1.3. Determination of IC_{50} Value (MTT Assay).

After plating 5000 cells per well in 96-well plates, the cells were preincubated in drug-free media at 37 °C for 24 h before adding different concentrations of the compounds to be tested. In order to prepare the stock solution of the drug, the solid complex was dissolved in DMSO. This stock was further diluted using cell culture medium until working concentrations were achieved. The drug exposure period was 48 h. Subsequently, 15 μL of 5 mg mL^{-1} MTT solution was added to form a

purple formazan. Afterwards, 100 μL of dimethyl sulfoxide (DMSO) was transferred into each well to dissolve the purple formazan, and results were measured using a microplate reader (DNM-9606, Perlong Medical, Beijing, China) at an absorbance of 570 nm. Each well was triplicated and each experiment repeated at least three times.

1.4. BSA Binding Experiments.

The titration experiments including UV-Vis absorption and fluorescence quenching were performed at constant concentration of BSA. A BSA stock solution was prepared in Tris buffer (5 mM Tris-HCl/10 mM NaCl at pH 7.2) and stored at 4 °C. All spectra were recorded after each successive addition of the complexes and incubation at room temperature for 5 min to complete the interaction. In the UV-Vis absorption titration experiment, a BSA solution (2.5 mL, 10 μM) was titrated by successive additions of the stock solutions of complexes and the changes in the BSA absorption were recorded after each addition. The fluorescence emission spectra of BSA in the absence and presence of the complexes were also recorded with excitation at 288 nm. The concentrations of the complexes were 0-10 μM, and the concentration of BSA was fixed at 10 μM. Synchronous fluorescence spectra of BSA with various concentrations of complexes (0-10 μM) were obtained from 220 to 340 nm when $\Delta\lambda$ = 60 nm and from 240 to 340 nm when $\Delta\lambda$ = 15 nm.

1.5. ROS Determination.

ROS production was measured with an ROS assay kit according to the manufacturer's instructions. A portion of 1×10^6 cells/mL was seeded in 6-well culture plates, treated with three different concentrations of the complexes, and incubated at 37 °C with 5% CO_2 for 24 h. After treatment with these drugs the cells were stained with 10 μM DCFH-DA solution (stock concentration 10 mM in DMSO) and incubated at 37 °C for 30 min and images were taken with a fluorescence

microscope after incubation. Relative ROS production was calculated versus the control.

1.6. Measurement of Lipophilicity (log $P_{o/w}$).

The octanol-water partition coefficients (*P*) of **Ir1** and **Ir7** were determined using a shake-flask method. Water (50 mL, distilled after milli-Q purification) and 1-octanol (50 mL, vacuum distilled) were shaken together using a laboratory shaker, for 72 h to allow saturation of both phases. Stock solutions of these complexes (50 μM) were prepared in the aqueous phase and aliquots (5 mL) of each of these stock solutions were then added to an equal volume of the 1-octanol phase. The resultant biphasic solutions were mixed for 2 h and then centrifuged (3000 × g, 5 min) to separate the phases. The concentrations of these complexes in the organic and aqueous phases were then determined using UV-vis (260 nm). Log $P_{o/w}$ was defined as the logarithm of the ratio of the concentrations of the complex in the organic and aqueous phases (values reported are the means of three separate determinations)

1.7. Induction of Apoptosis.

Flow cytometry analysis of apoptotic populations of A549 cells and A549/DDP cells caused by exposure to complexes **Ir1** and **Ir7** were carried out using the Annexin V-FITC Apoptosis Detection Kit (Beyotime Institute of Biotechnology, China) according to the supplier's instructions. Briefly, 1.5×10^6 A549 or A549/DDP cells per well were seeded in a six-well plate. Cells were preincubated in drug-free media at 37 °C for 48 h, after which drugs were added at concentrations of $0.25 \times IC_{50}$, $0.5 \times IC_{50}$ and $1 \times IC_{50}$. After 48 h of drug exposure, cells were collected, washed once with PBS, and resuspended in 195 μL of annexin V-FITC binding buffer which was then added to 5 μL of annexin V-FITC and 10 μL of PI, and then incubated at room temperature in the dark for 15 min. Subsequently, the buffer placed in an ice bath in the dark. The

samples were analyzed by a flow cytometer (ACEA NovoCyte, Hangzhou, China). Cells for apoptosis studies were used with no previous fixing procedure as to avoid nonspecific binding of the annexin V-FITC conjugate.

1.8. Cell Cycle Analysis.

A549 cells at 1.5 × 10^6 per well were seeded in a six-well plate. Cells were preincubated in drug-free media at 37 °C for 24 h, after which drugs were added at concentrations of 0.25 × IC_{50} and 0.5 × IC_{50} of complexes **Ir1** and **Ir7** were against A549 cancer cells. After 24 h of drug exposure, supernatants were removed by suction and cells were washed with PBS. Finally, cells were harvested using trypsin-EDTA and fixed for 24 h using cold 70% ethanol. DNA staining was achieved by resuspending the cell pellets in PBS containing propidium iodide (PI) and RNAse. Cell pellets were washed and resuspended in PBS before being analyzed in a flow cytometer (ACEA NovoCyte, Hangzhou, China) using excitation of DNA-bound PI at 488 nm, with emission at 585 nm. Data were processed using NovoExpress software. The cell cycle distribution is shown as the percentage of cells containing G_0/G_1, S and G_2/M DNA as identified by propidium iodide staining.

1.9. Cellular Uptake.

A549 cells were seeded in 6-well plates for 48 h and preincubated with CCCP (50 μM) or chloroquine (50 μM) for 1 h. The medium was removed and the cells were then incubated with **Ir1** and **Ir7** (2 μM) for 1 h. To investigate the impact of temperature on cellular uptake, the cells were incubated at 4 °C or 37 °C for 1 h. In each case, the cells were washed three times with ice-cold PBS and visualize by confocal microscopy (LSM 880 NLO, Carl Zeiss, Göttingen, Germany) immediately.

1.10. Colocalization Assay.

A549 cells were incubated with **Ir1** and **Ir7** (2 μM) for 1 h at 37 ºC, then co-incubated with DAPI (1 μg/mL), MTDR (500 nM) and LTDR (75 nM) for 1 h, respectively. **Ir1** and **Ir7** were excited at 488 nm and the emission was collected at 490-590 nm. DAPI was excited at 345 nm and the emission was collected at 410-455 nm; MTDR was excited at 644 nm and the emission was collected at 660-720 nm; LTDR was excited at 594 nm and the emission was collected at 600-660 nm. Cells were washed three times with PBS and visualized by confocal microscopy (LSM 880 NLO, Carl Zeiss, Göttingen, Germany).

1.11. Inhibition of Cell Migration.

A549 cells (1,500,000 per well) were seeded in 2000 μL media in 6-well plates and allowed to attach and grow to form a confluent monolayer. Each well of the plates was marked with a horizontal line passing through the center of bottom in advance. Wounds were created perpendicular to the lines by 10 μL tips, and unattached cells were removed by washing with PBS (pH = 7.4). **Ir1** and **Ir7** in DMEM with 1% PBS was added and cells incubated at 37 ºC under 5% CO_2 for imaging. DMEM with 1% PBS was used to suppress cell proliferation. Images were captured at 0 and 24 h at the same position of each well. Experiments were repeated for at least three times.

1.12. Statistical Analysis.

Data are expressed as means ± standard deviation. The statistically significant difference between data means was determined by the student *t*-test. $P < 0.05$ indicated a statistically significant difference.

1.13. Mitochondrial Membrane Assay.

Analysis of the changes of mitochondrial potential in A549 cells after exposure to **Ir1** and **Ir7** were carried out using the Abcam, JC-1 mitochondrial membrane potential assay kit according to the manufacturer's instructions. The JC-1 dye emits red fluorescence (λ_{ex} = 575 nm, λ_{em} = 590 nm) when the mitochondrial membrane is intact with the usual $\triangle\psi_m$ (since JC-1 remains in aggregates) and when the membrane potential is no longer intact it emits green fluorescence (λ_{ex} = 510 nm, λ_{em} = 550 nm) due to the monomeric form. Therefore, a decrease in the ratio of the red/green fluorescence intensity of JC-1 reflects depolarization of the mitochondrial membrane potential. Briefly, 1.5 × 10^6 cells were seeded in six-well plates left to incubate for 24 h in drug-free medium at 310 K in a humidified atmosphere. Drug solutions, at equipotent concentrations equal to 0.5 × IC_{50}, 1 × IC_{50} and 2 × IC_{50} were added in triplicate, and the cells were left to incubate for a further 24 h under similar conditions. These concentrations are obtained via dilution of ca. 10 mM DMSO stock solutions. The percentage of DMSO each solution is in the range of 0.005% to 0.028% (v/v). The corresponding concentration of DMSO in the negative control is 0.028% (v/v). Supernatants were removed by suction, and each well was washed with PBS before detaching the cells using trypsin-EDTA. Staining of the samples was done in flow cytometry tubes protected from light, incubating for 30 min at ambient temperature. The samples were immediately analyzed by a flow cytometer (ACEA NovoCyte, Hangzhou, China). For positive controls, the cells were exposed to carbonyl cyanide 3-chlorophenylhydrazone, CCCP (5 μM), for 20 min. Data were processed using NovoExpress™ software. Each sample was triplicated and each experiment repeated three times.

1.14. Lysosomal Damage.

A549 cells seeded into six-well plate (Corning) were exposed to complexes **Ir1** and **Ir7** at the

indicated concentrations for 12 h. The cells were then washed twice with PBS and incubated with AO (5 μM) at 37 ºC for 15 min. The cells were washed twice with PBS and visualized by confocal microscopy (LSM/880NLO). Emission was collected at 510 ± 20 nm (green) and 625 ± 20 nm (red) upon excitation at 488 nm.

1.15. Inductively coupled plasma mass spectrometry (ICP-MS).

A549 cells were seeded in 90 mm dishes for 24 h (three dishes were prepared per compound tested). The media was removed and replaced with fresh media containing the tested complex (5 μM) for 48 h. After the removal of the culture media and rinse with 1 mL of PBS buffer (1x), the cells were treated with 500 μL of 0.25% trypsin and centrifuged at 1000 rpm. The cells were centrifuged, quickly washed with PBS, and stored at 253 K for determination of total cell accumulation of metal complex. The samples were nitrolysis with concentrated HNO_3 at 95 ℃ for 2 h, H_2O_2 at 95 ℃ for 1.5 h and concentrated HCl at 37 ℃ for 0.5 h. Finally, the solution was diluted to 2 mL with MQ water and the metal content was measured by the inductively coupled plasma mass spectrometer (ICP-MS; VG Elemental).

2. FIGURES

2.1. ^{1}H and ^{13}C NMR Spectra Datas.

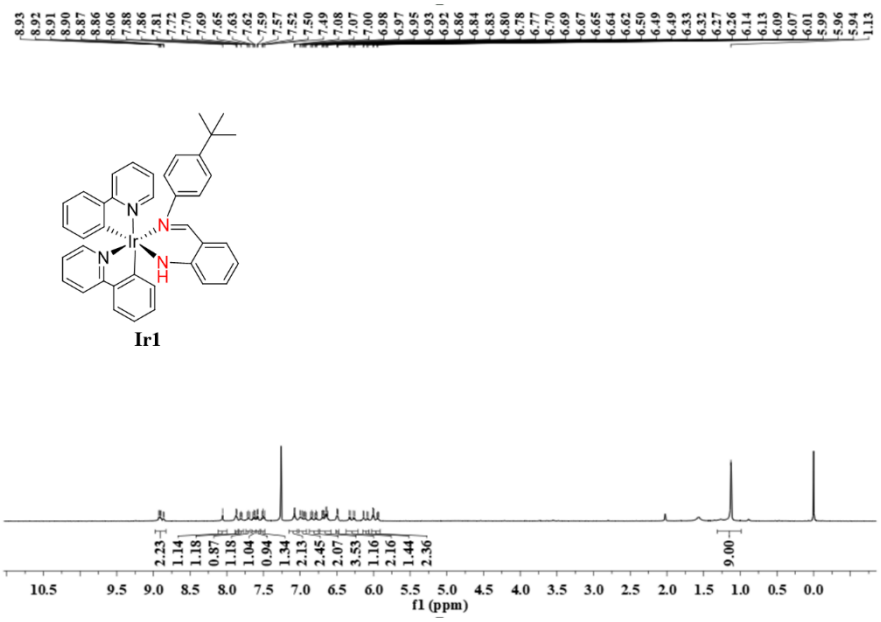

Figure S1. ^{1}H NMR spectrum of **Ir1** in $CDCl_3$.

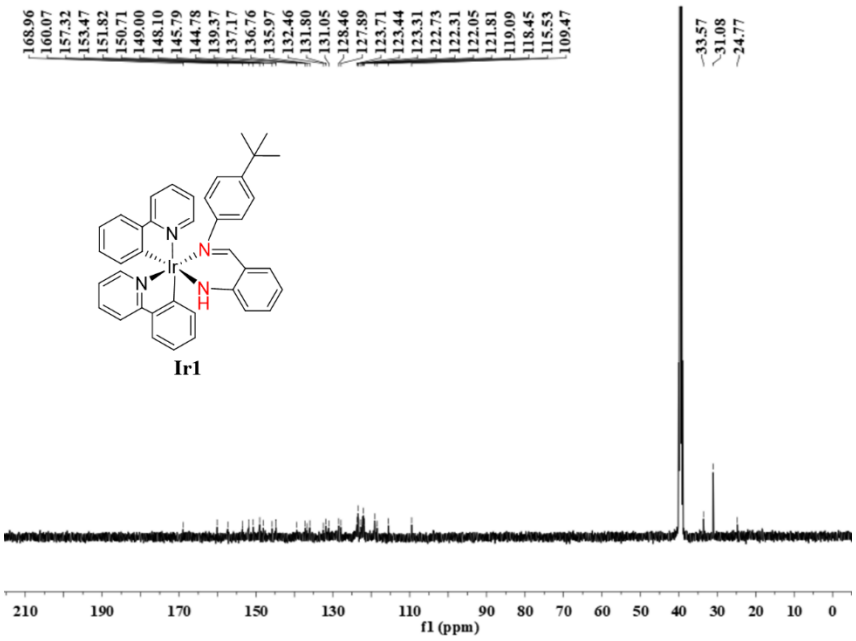

Figure S2. ^{13}C{^{1}H} NMR spectrum of **Ir1** in DMSO-d_6.

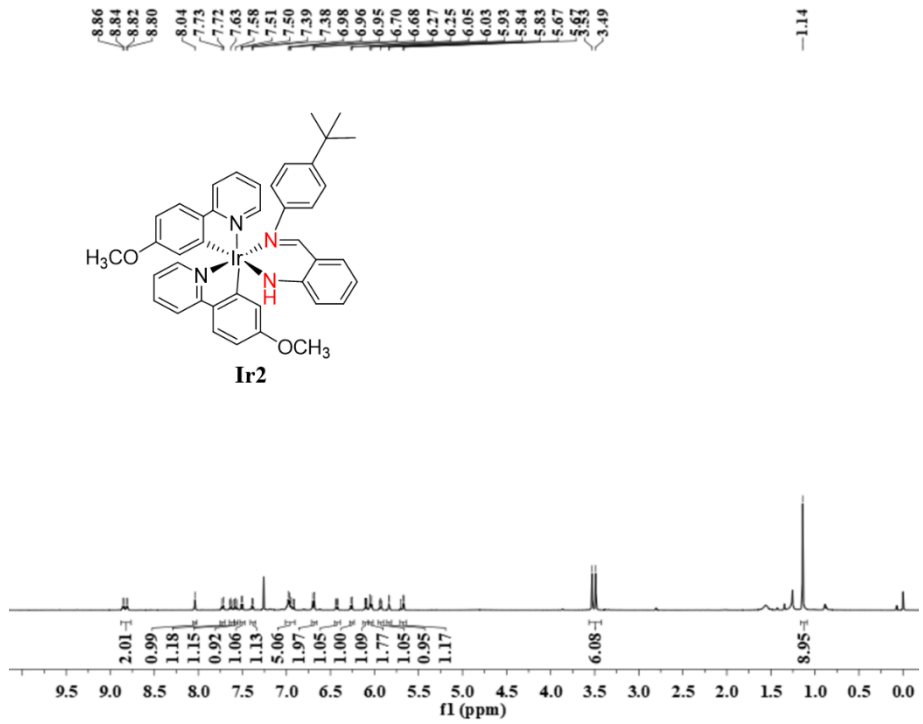

Figure S3. ^{1}H NMR spectrum of **Ir2** in $CDCl_3$.

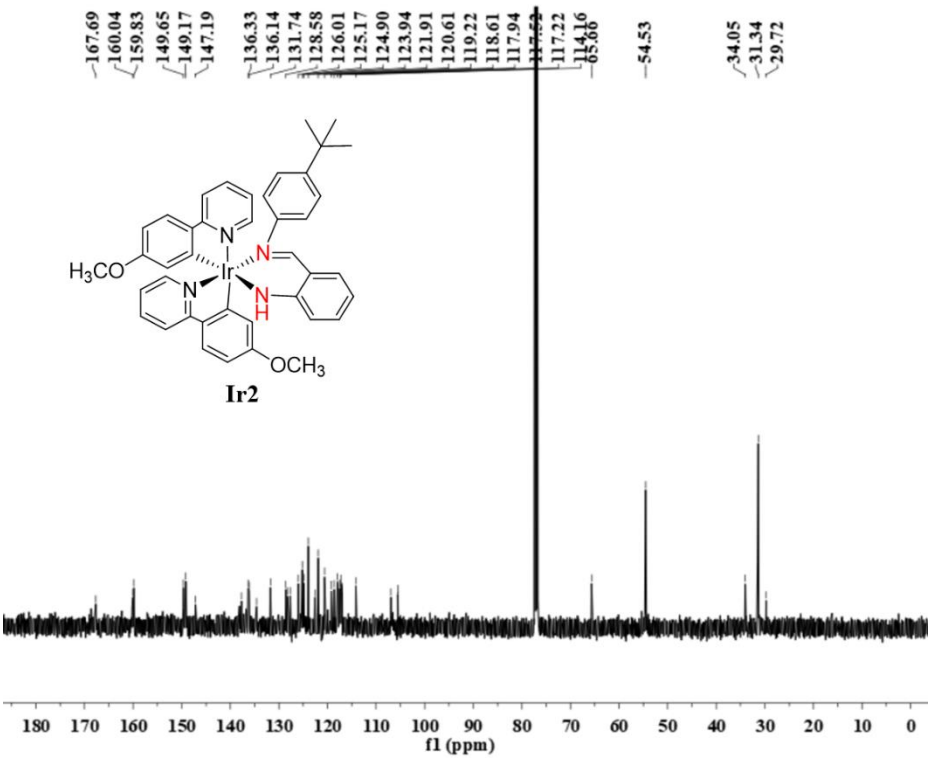

Figure S4. $^{13}C\{^{1}H\}$ NMR spectrum of **Ir2** in $CDCl_3$.

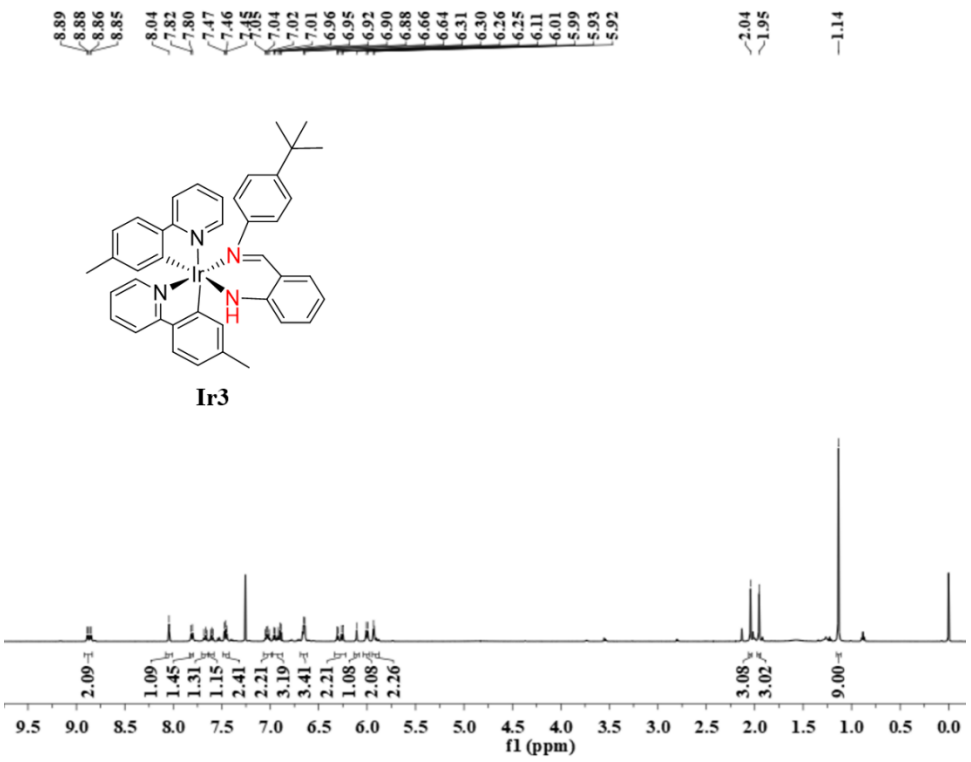

Figure S5. ^{1}H NMR spectrum of **Ir3** in $CDCl_3$.

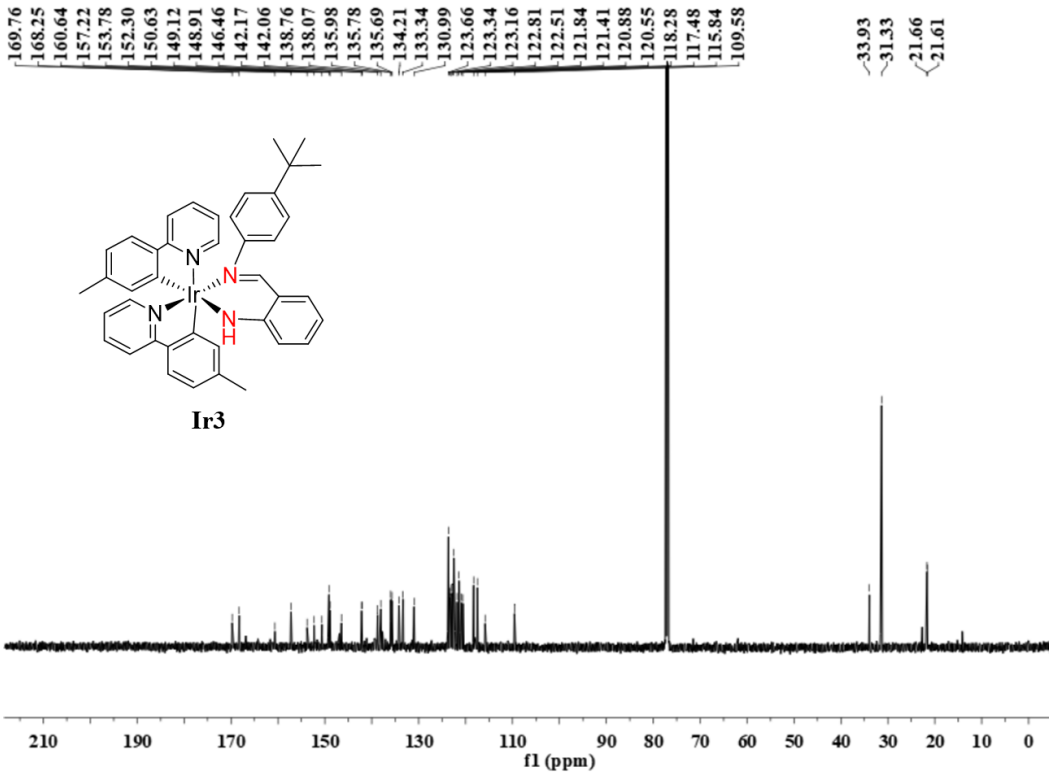

Figure S6. $^{13}C\{^{1}H\}$ NMR spectrum of **Ir3** in $CDCl_3$.

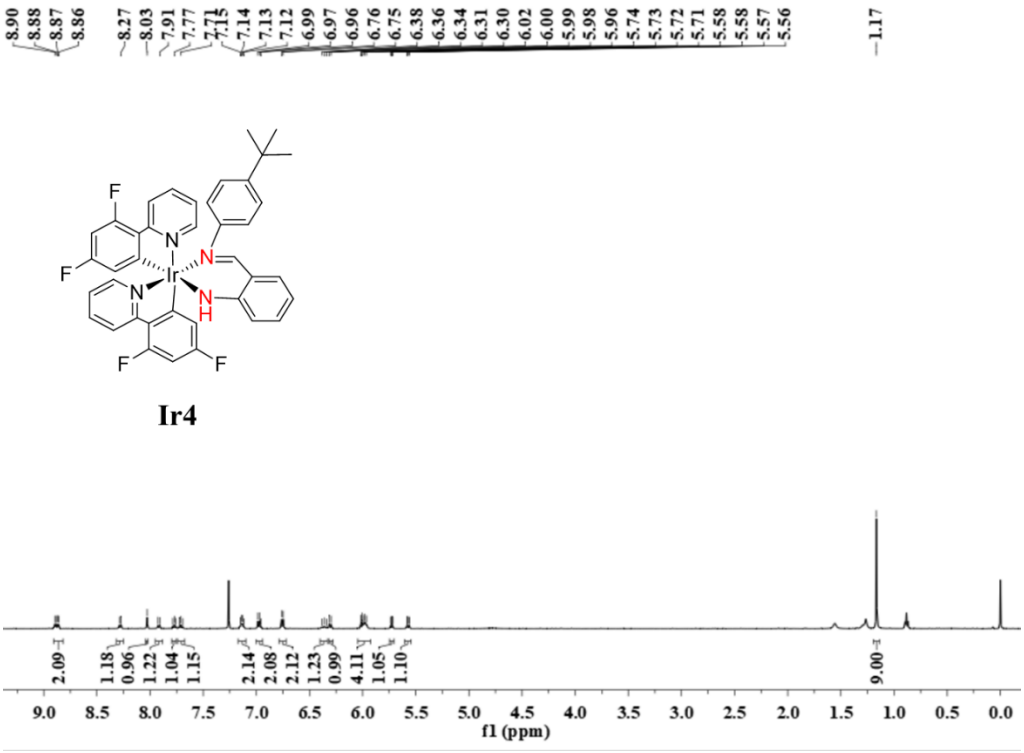

Figure S7. ^{1}H NMR spectrum of **Ir4** in $CDCl_3$.

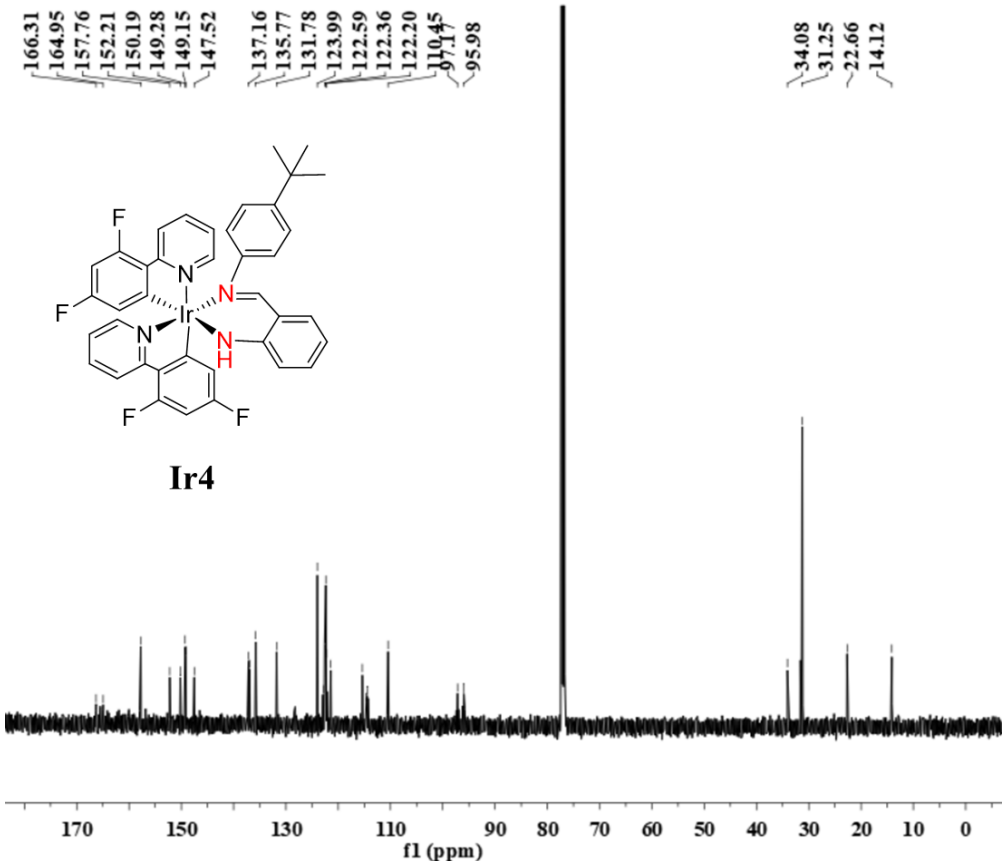

Figure S8. $^{13}C\{^{1}H\}$ NMR spectrum of **Ir4** in $CDCl_3$.

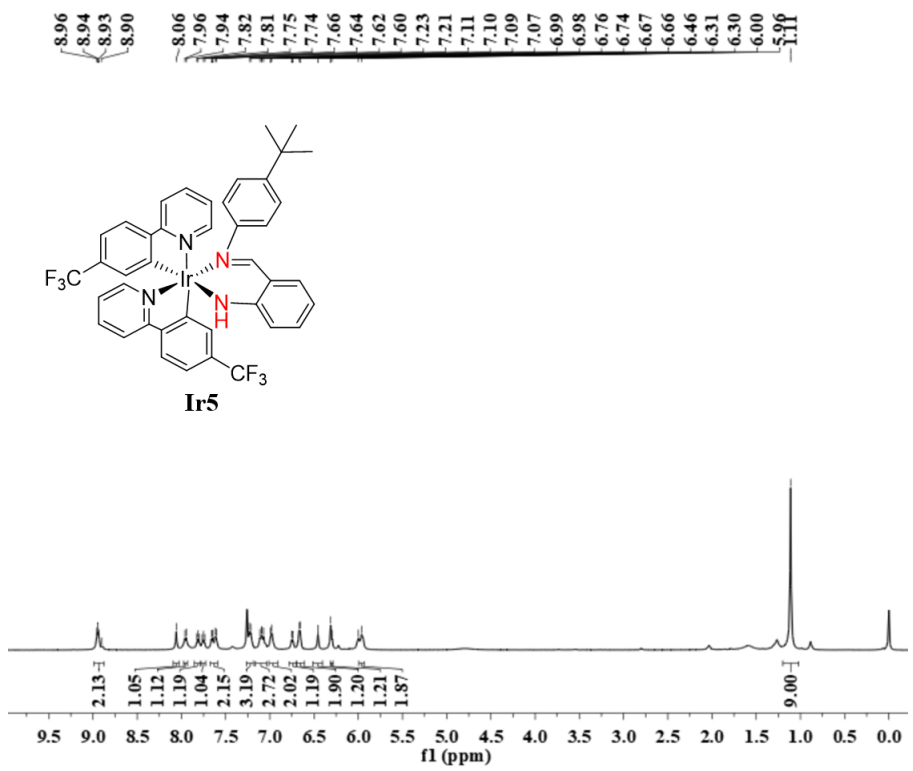

Figure S9. ^{1}H NMR spectrum of **Ir5** in $CDCl_3$.

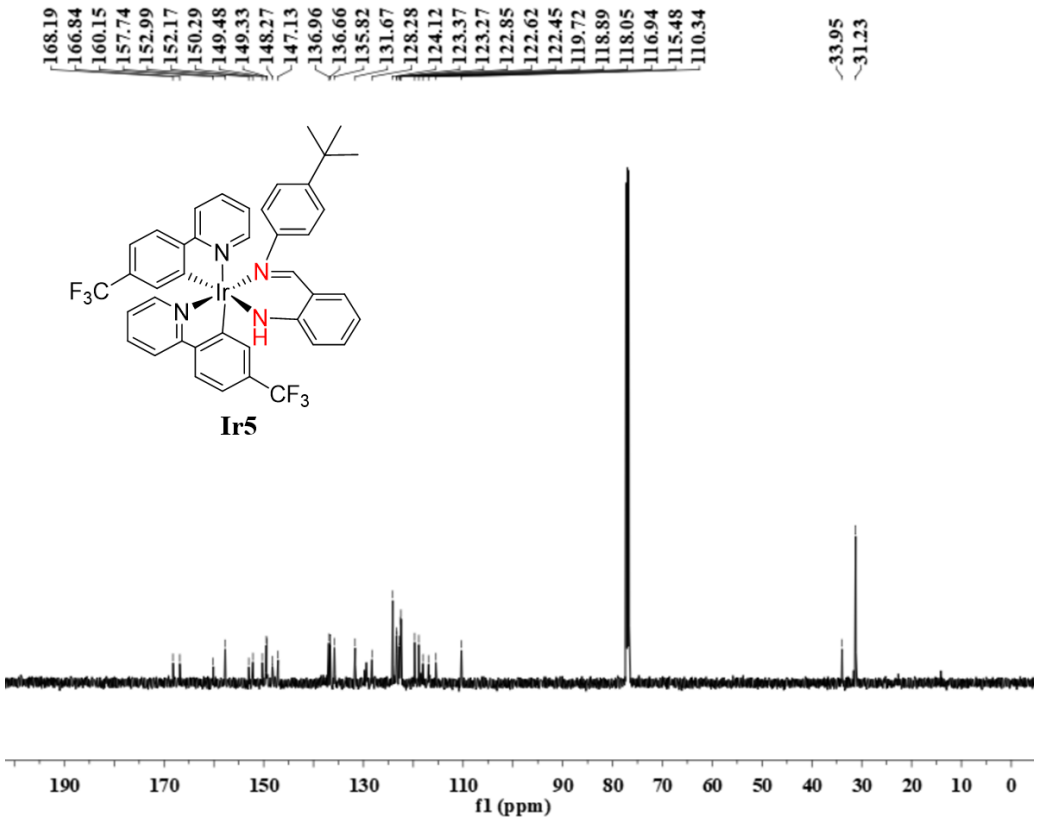

Figure S10. $^{13}C\{^{1}H\}$ NMR spectrum of **Ir5** in $CDCl_3$.

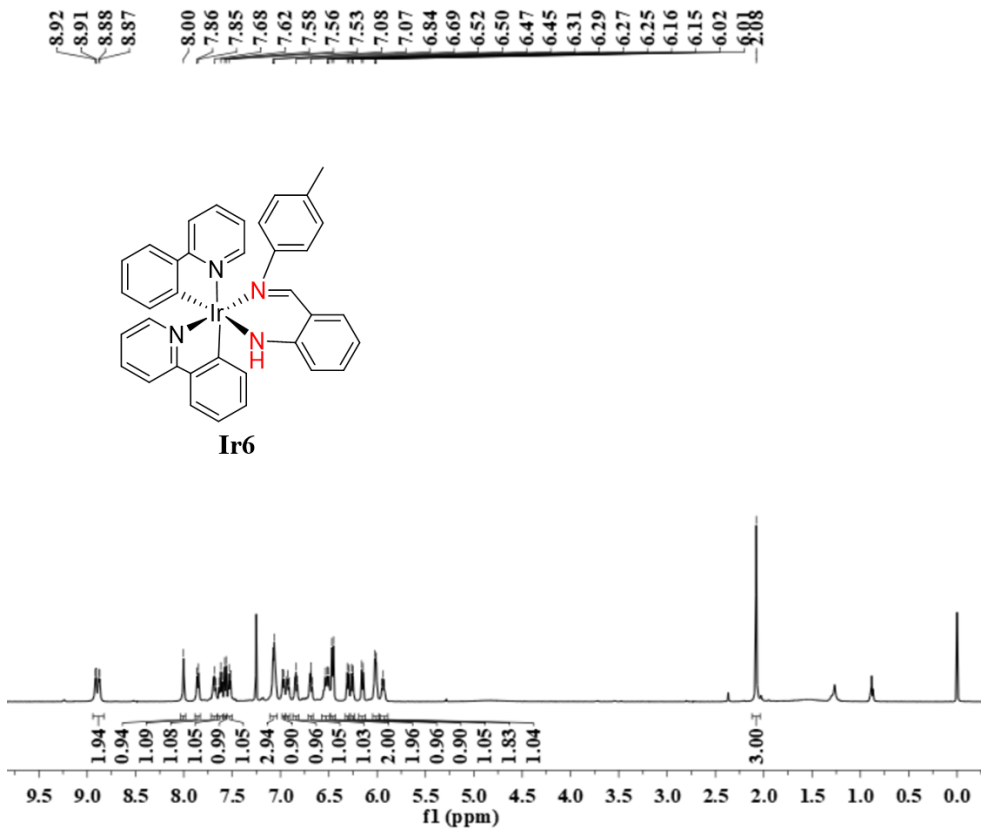

Figure S11. ^{1}H NMR spectrum of **Ir6** in $CDCl_3$.

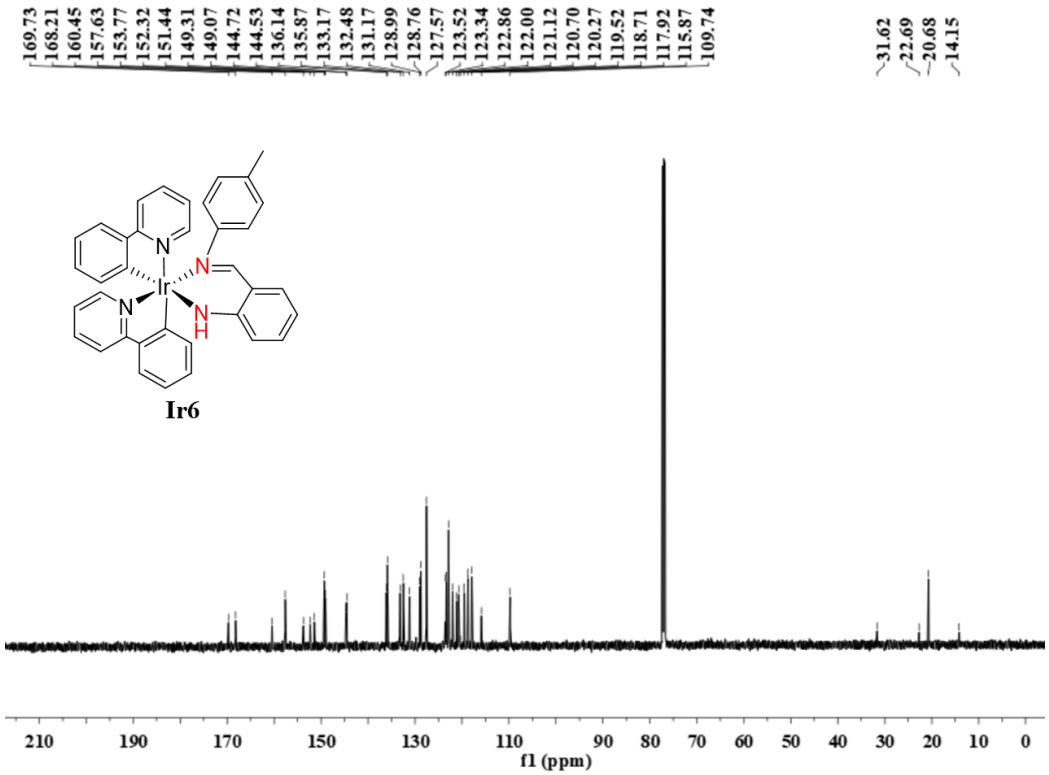

Figure S12. $^{13}C\{^{1}H\}$ NMR spectrum of **Ir6** in $CDCl_3$.

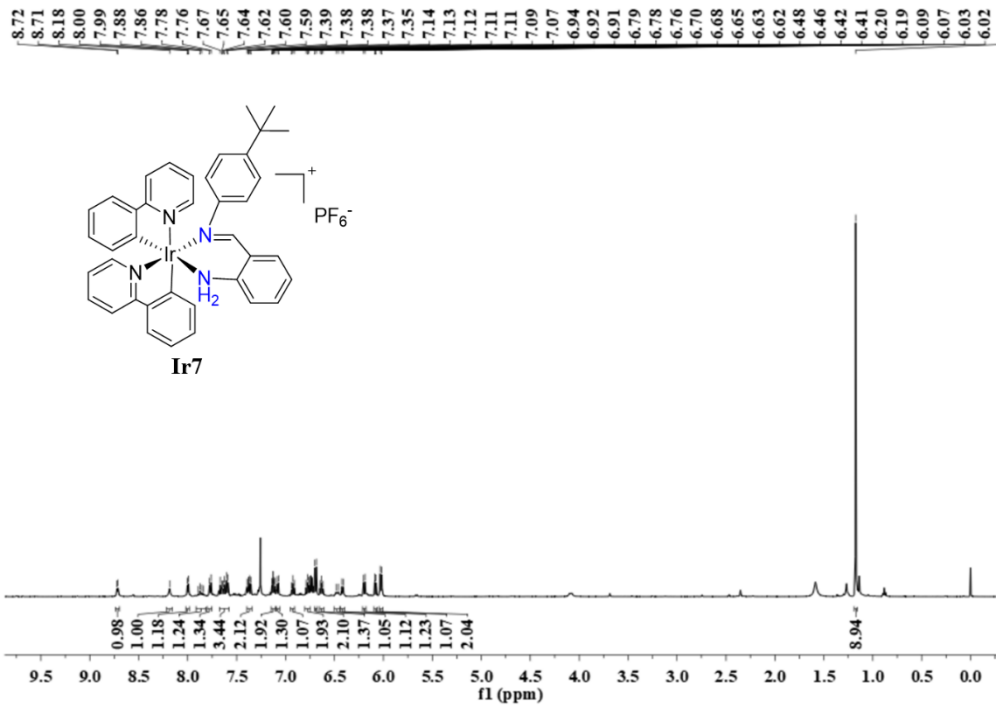

Figure S13. ^{1}H NMR spectrum of **Ir7** in $CDCl_3$.

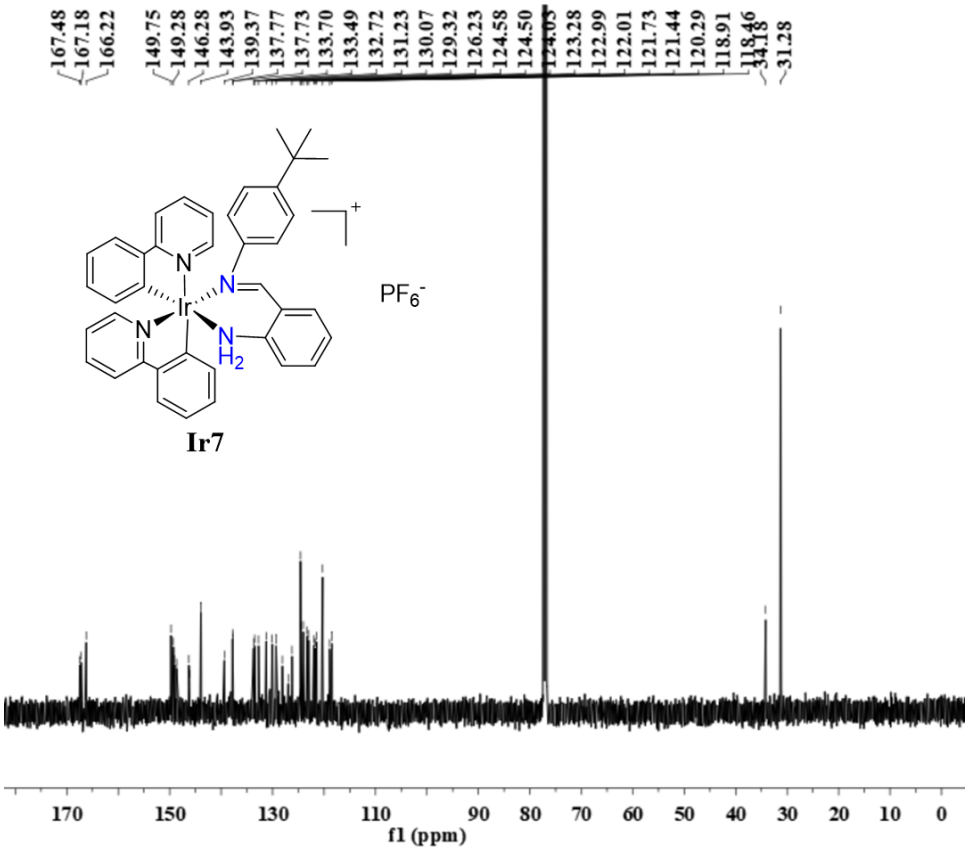

Figure S14. $^{13}C\{^{1}H\}$ NMR spectrum of **Ir7** in $CDCl_3$.

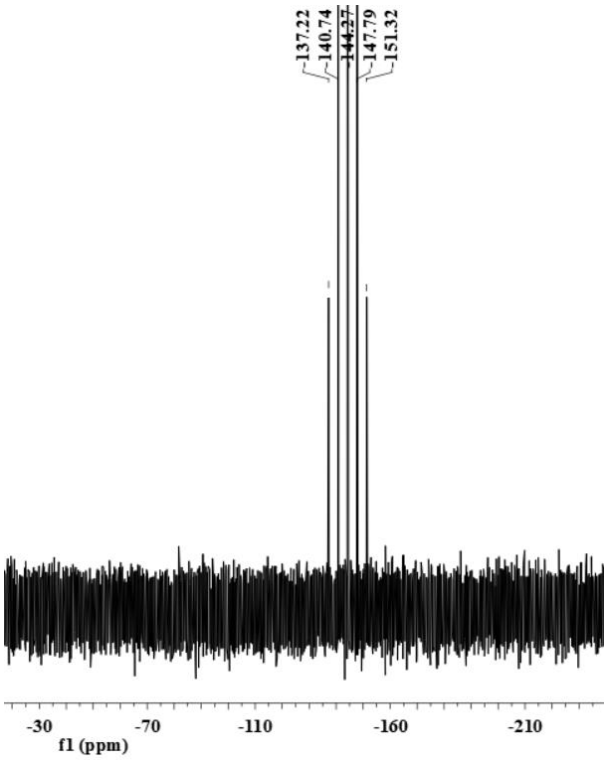

Figure S15. $^{31}P\{^{1}H\}$ NMR spectrum of **Ir7** in $CDCl_3$.

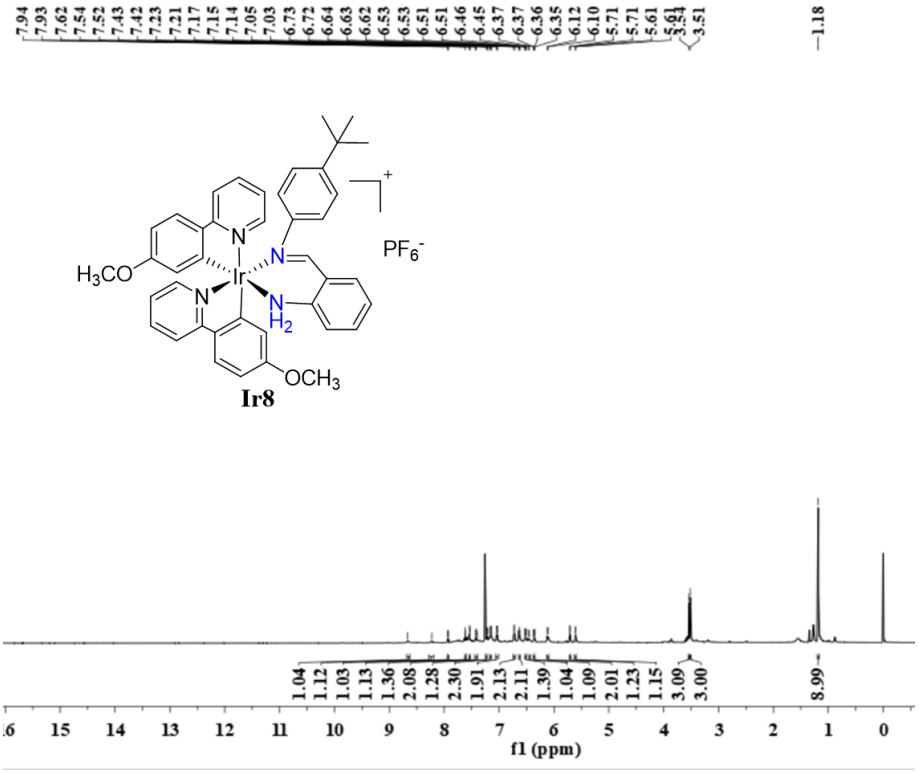

Figure S16. ^{1}H NMR spectrum of **Ir8** in $CDCl_3$.

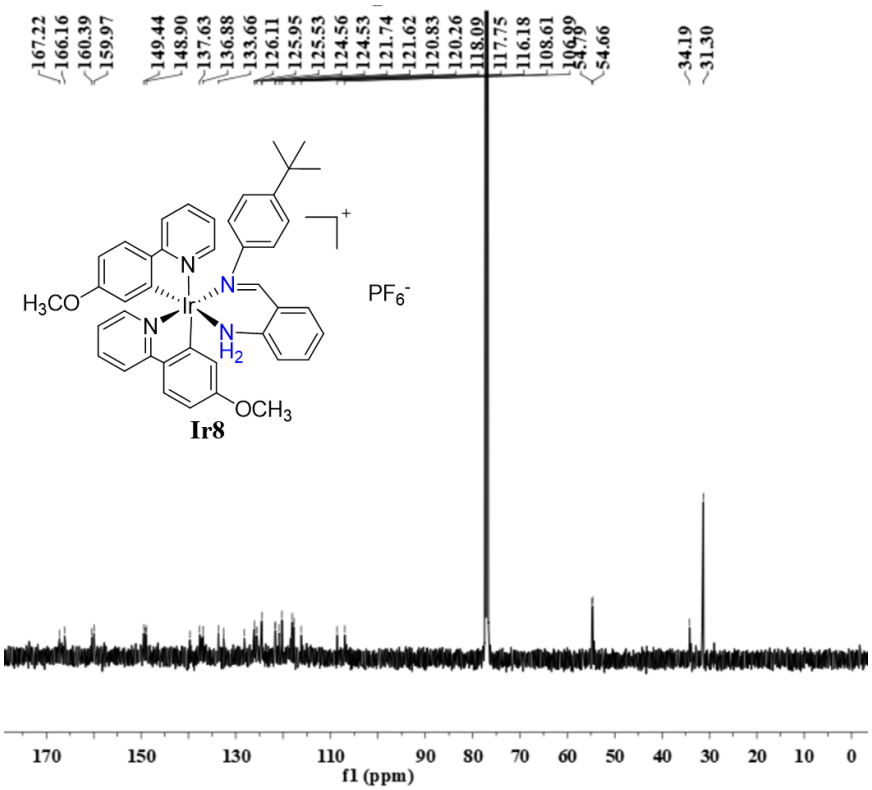

Figure S17. $^{13}C\{^{1}H\}$ NMR spectrum of **Ir8** in $CDCl_3$.

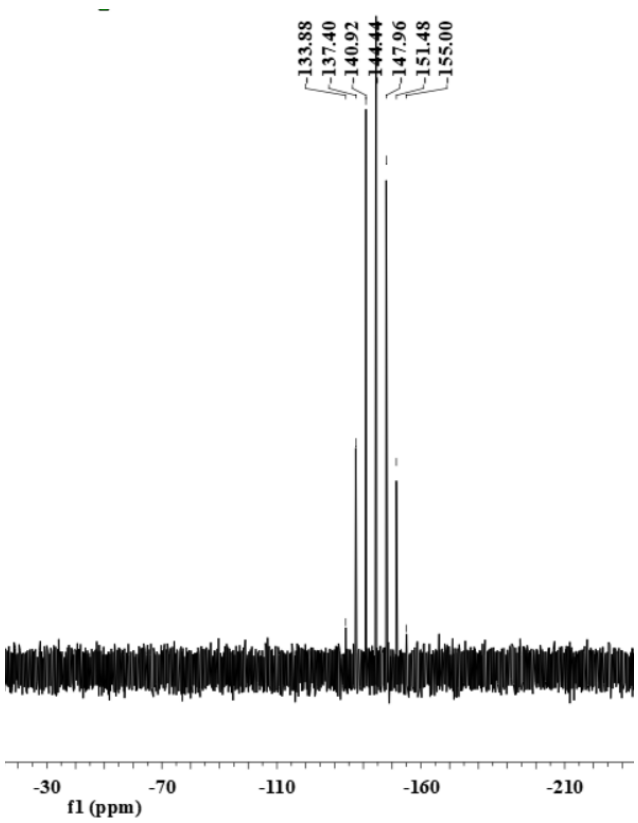

Figure S18. $^{31}P\{^{1}H\}$ NMR spectrum of **Ir8** in $CDCl_3$.

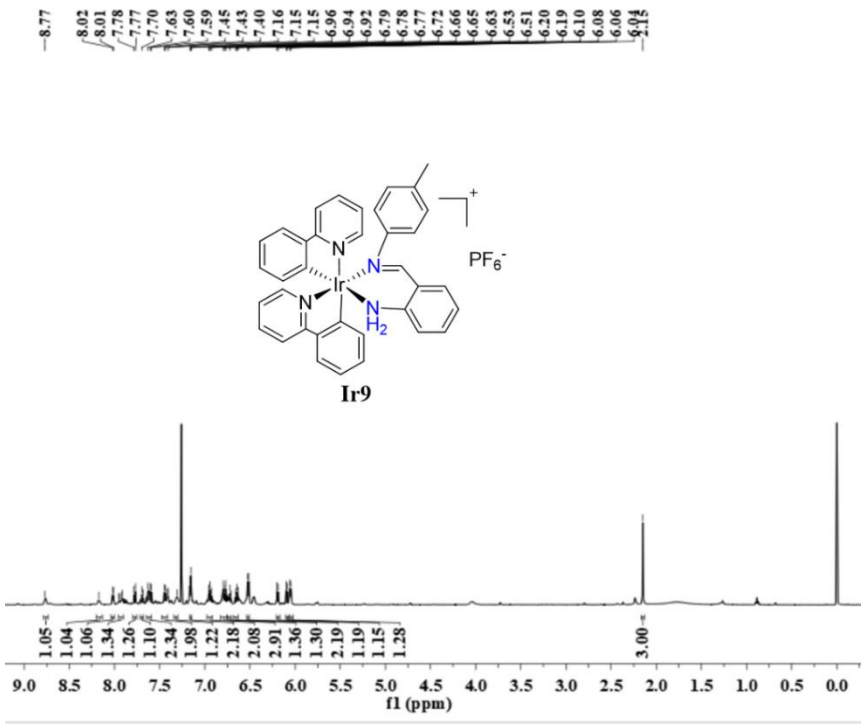

Figure S19. ^{1}H NMR spectrum of **Ir9** in $CDCl_3$.

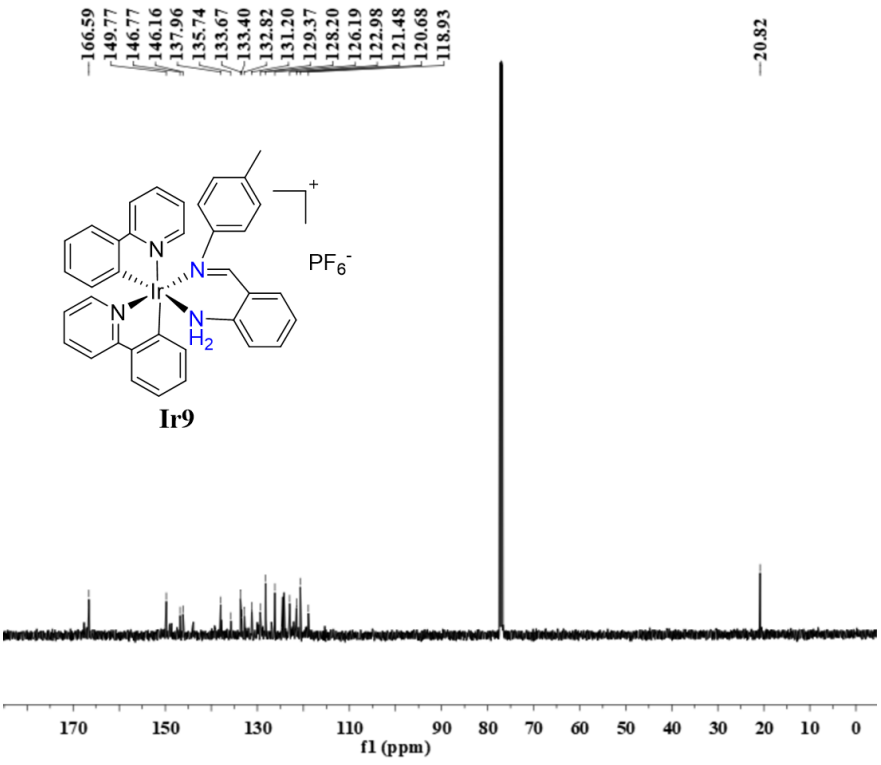

Figure S20. $^{13}C\{^{1}H\}$ NMR spectrum of **Ir9** in $CDCl_3$.

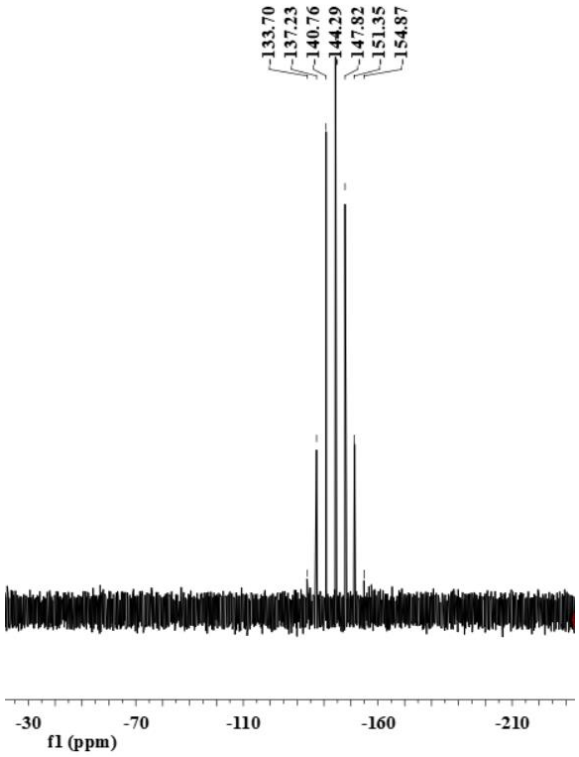

Figure S21. $^{31}P\{^{1}H\}$ NMR spectrum of **Ir9** in $CDCl_3$.

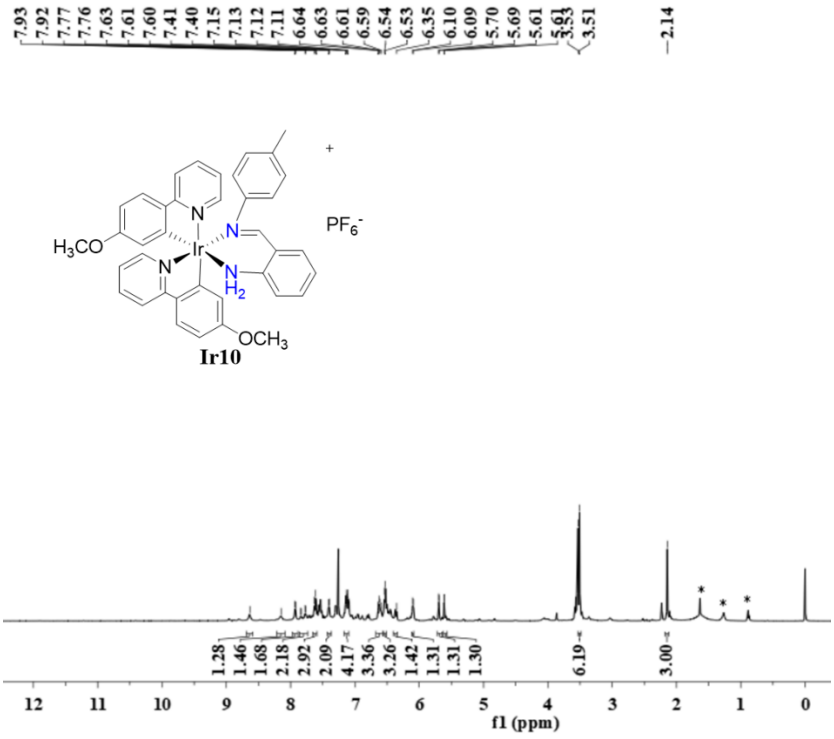

Figure S22. ^{1}H NMR spectrum of **Ir10** in $CDCl_3$. (* = H_2O and *n*-hexane)

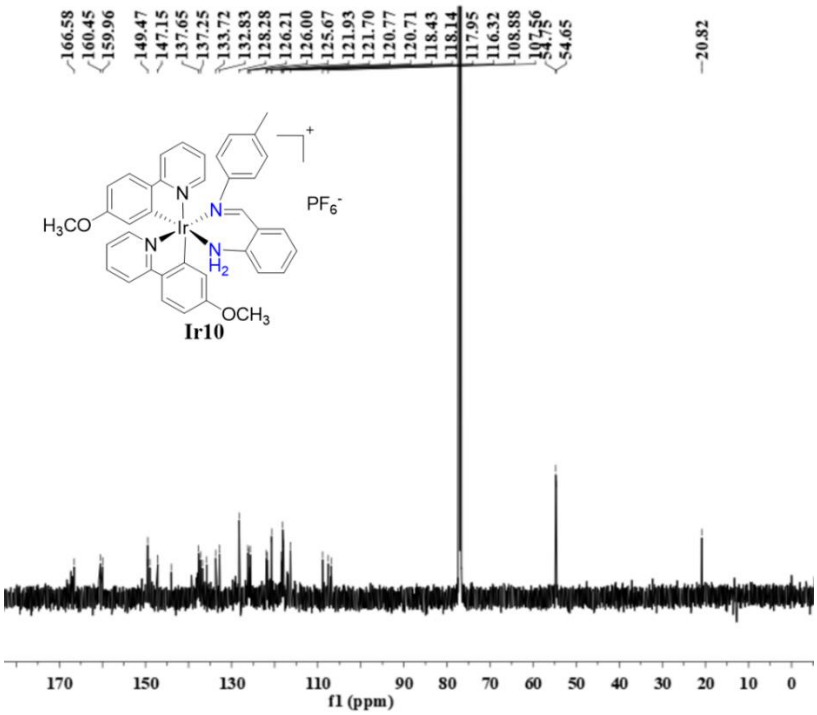

Figure S23. $^{13}C\{^{1}H\}$ NMR spectrum of **Ir10** in $CDCl_3$.

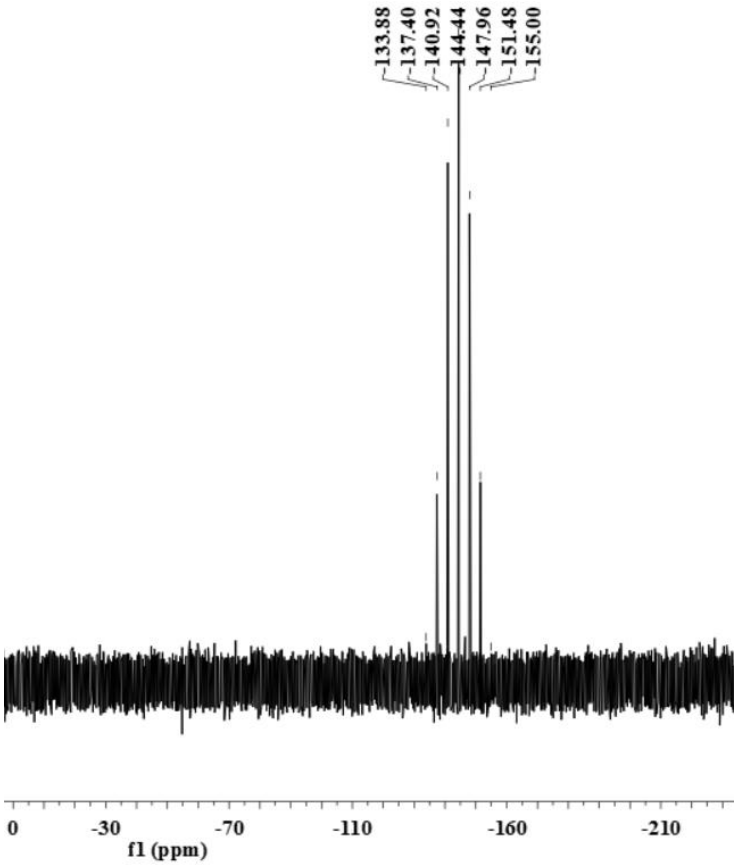

Figure S24. $^{31}P\{^{1}H\}$ NMR spectrum of **Ir10** in $CDCl_3$.

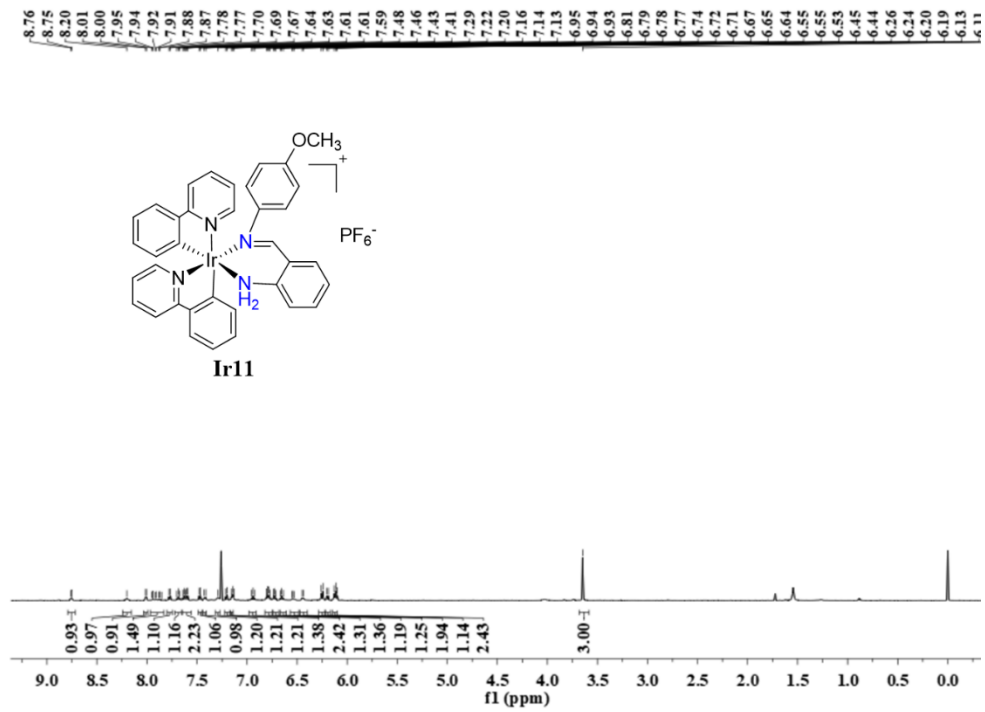

Figure S25. ^{1}H NMR spectrum of **Ir11** in $CDCl_3$.

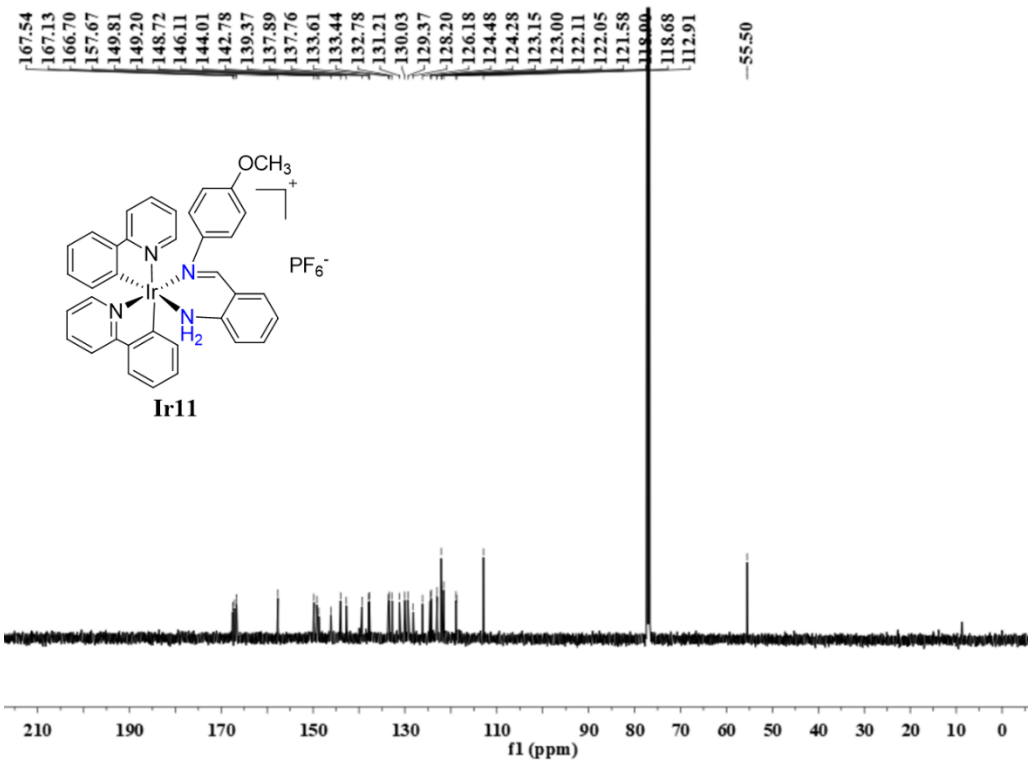

Figure S26. $^{13}C\{^{1}H\}$ NMR spectrum of **Ir11** in $CDCl_3$.

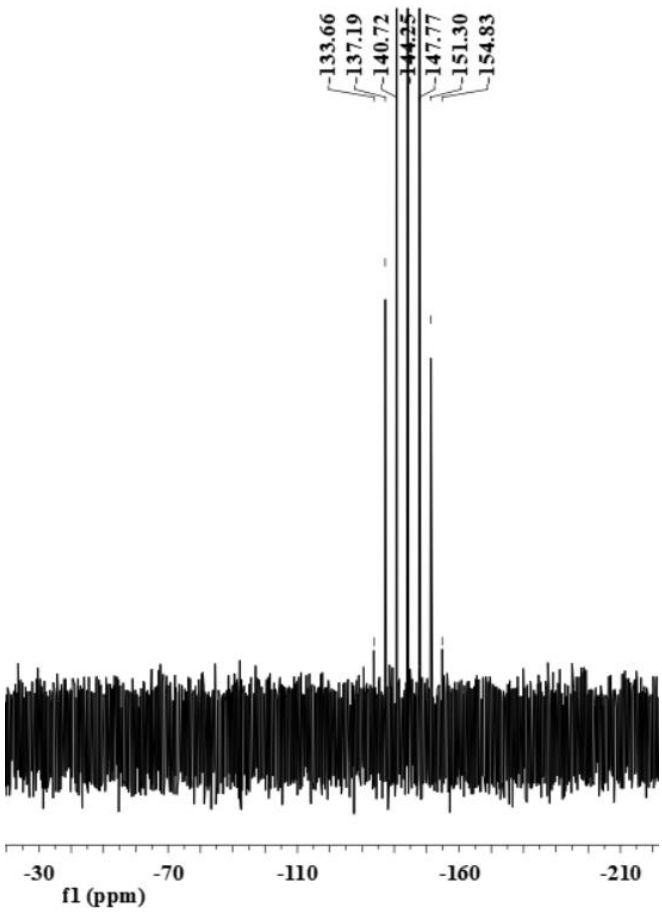

Figure S27. $^{31}P\{^{1}H\}$ NMR spectrum of **Ir11** in $CDCl_3$.

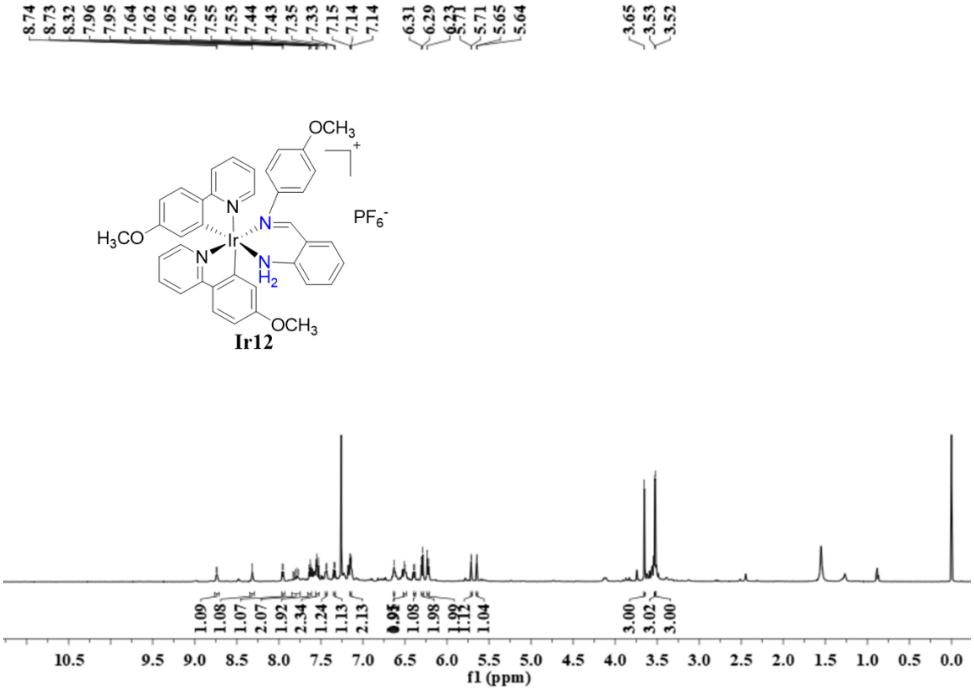

Figure S28. ^{1}H NMR spectrum of **Ir12** in $CDCl_3$.

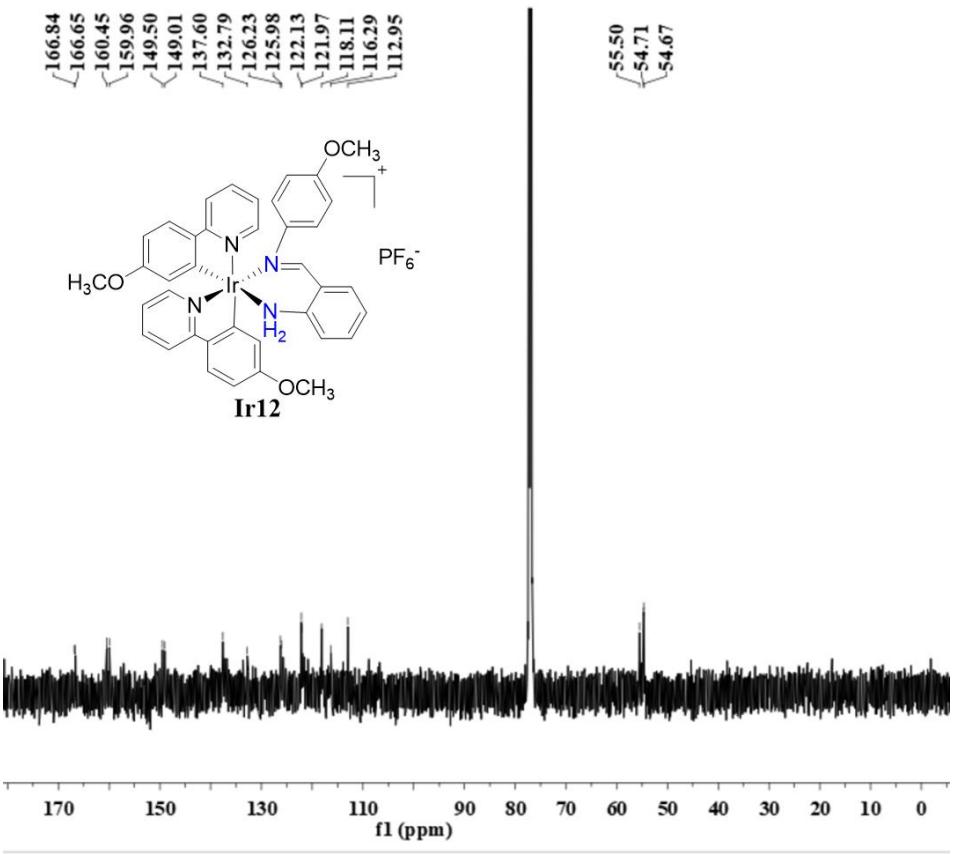

Figure S29. $^{13}C\{^{1}H\}$ NMR spectrum of **Ir12** in $CDCl_3$.

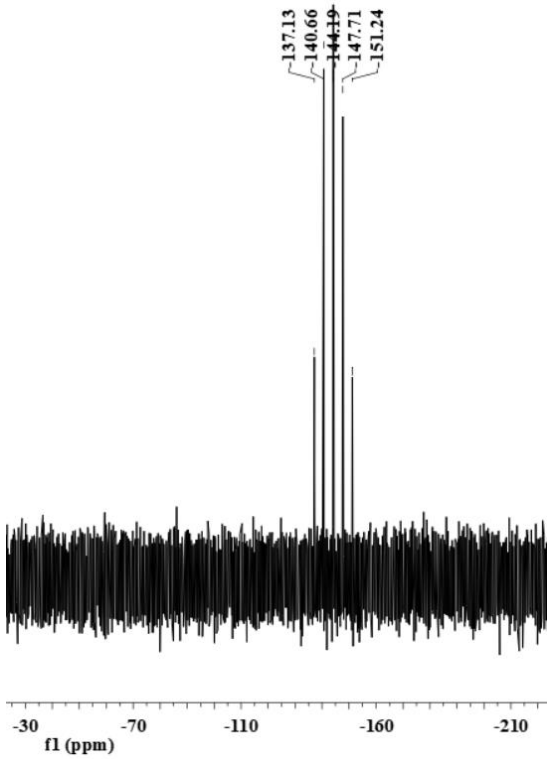

Figure S30. $^{31}P\{^{1}H\}$ NMR spectrum of **Ir12** in $CDCl_3$.

2.2. ESI-MS Data.

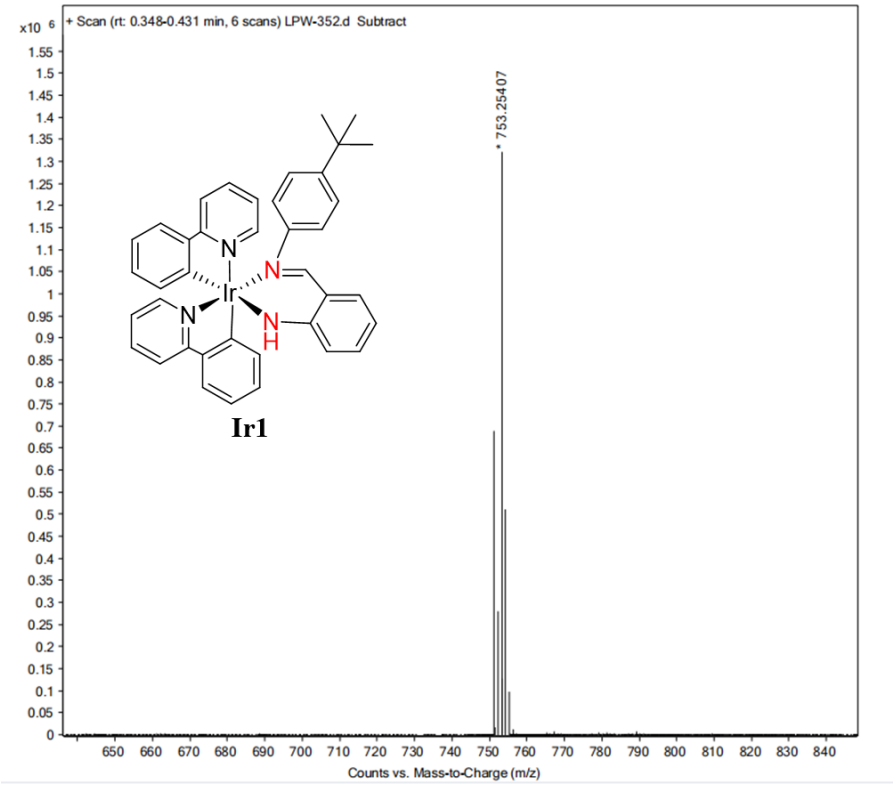

Figure S31. ESI-MS of **Ir1**.

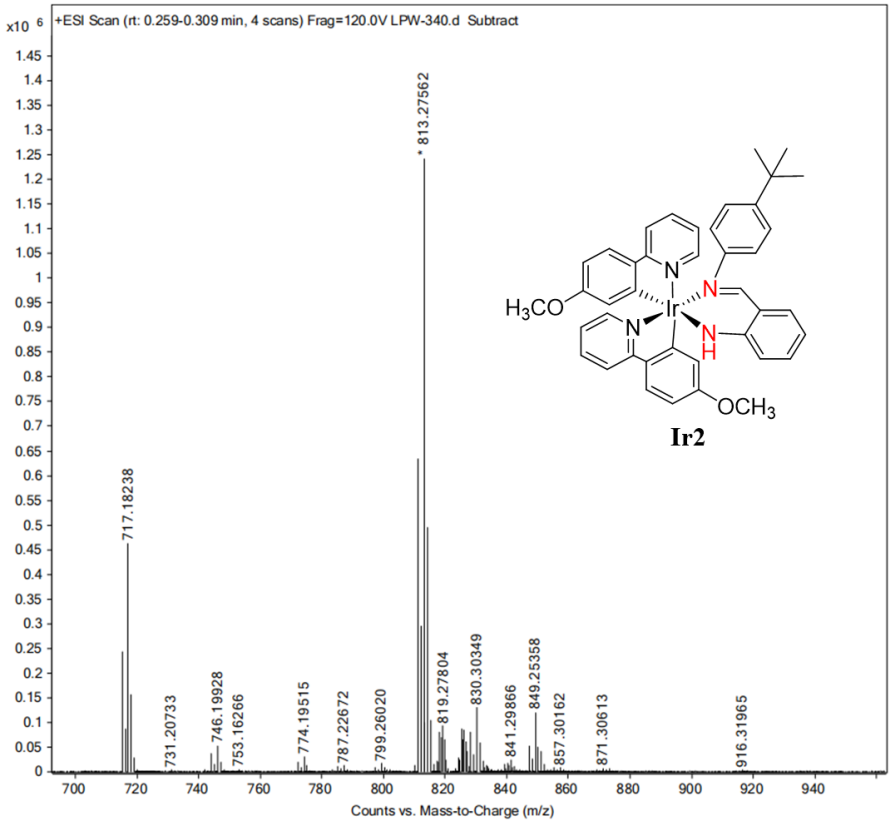

Figure S32. ESI-MS of **Ir2**.

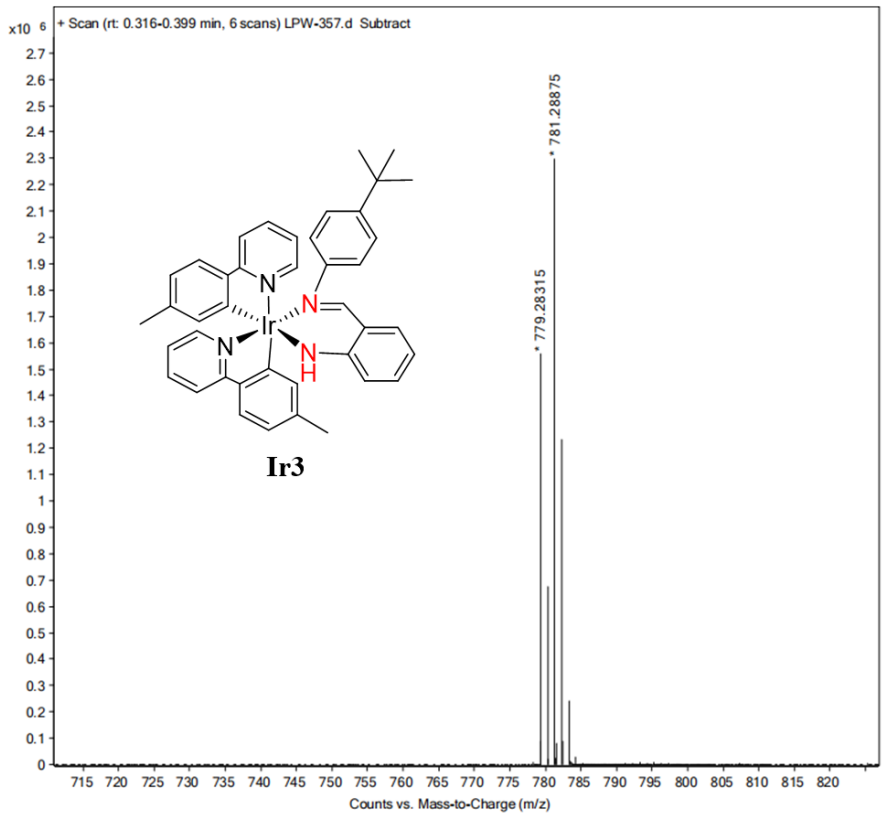

Figure S33. ESI-MS of **Ir3**.

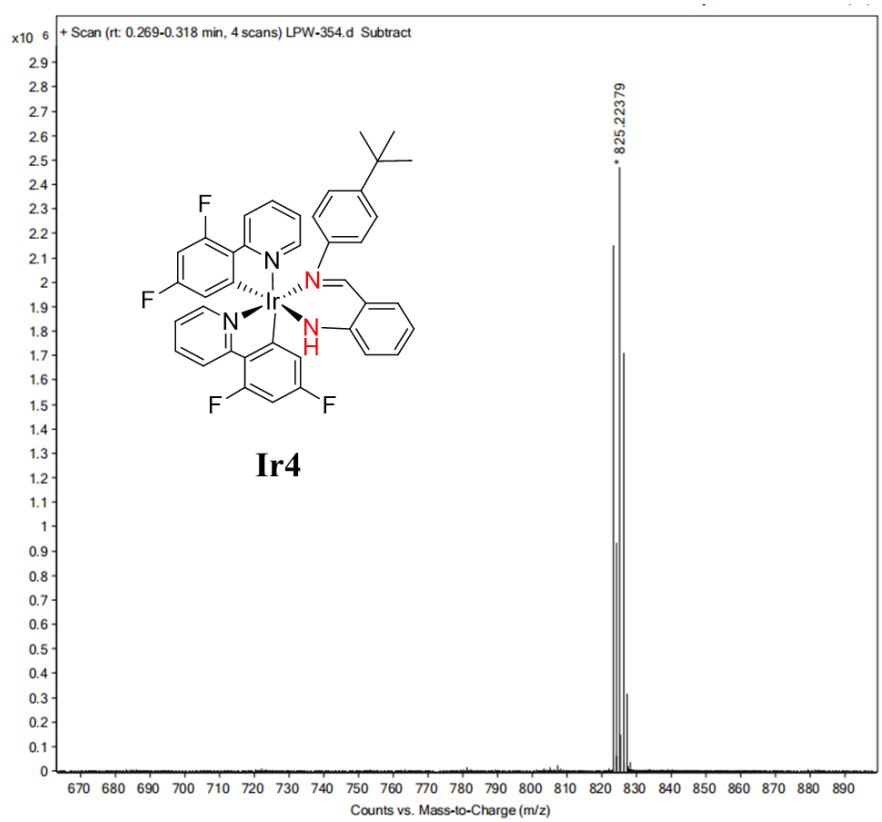

Figure S34. ESI-MS of **Ir4**.

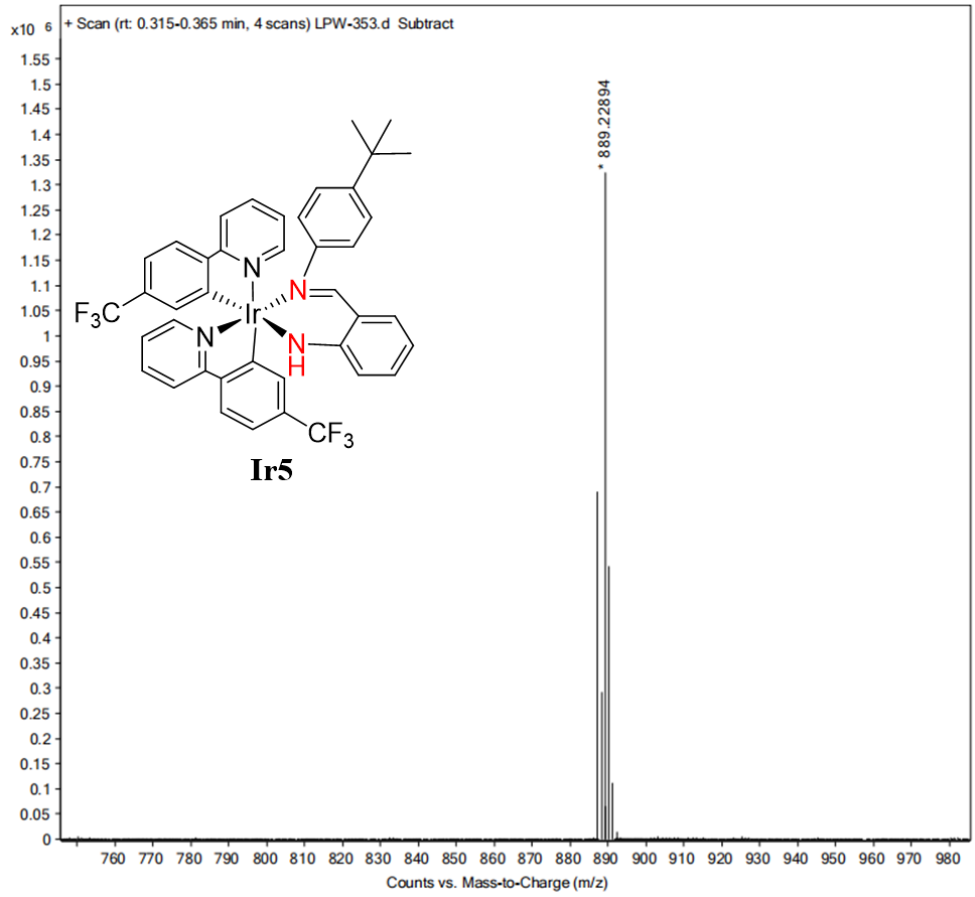

Figure S35. ESI-MS of **Ir5**.

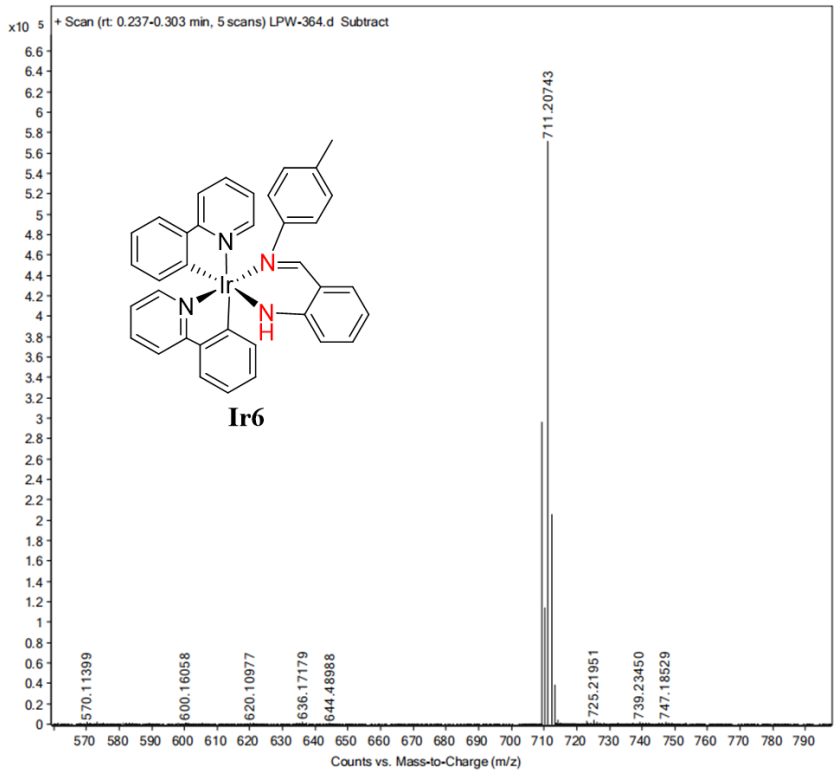

Figure S36. ESI-MS of **Ir6**.

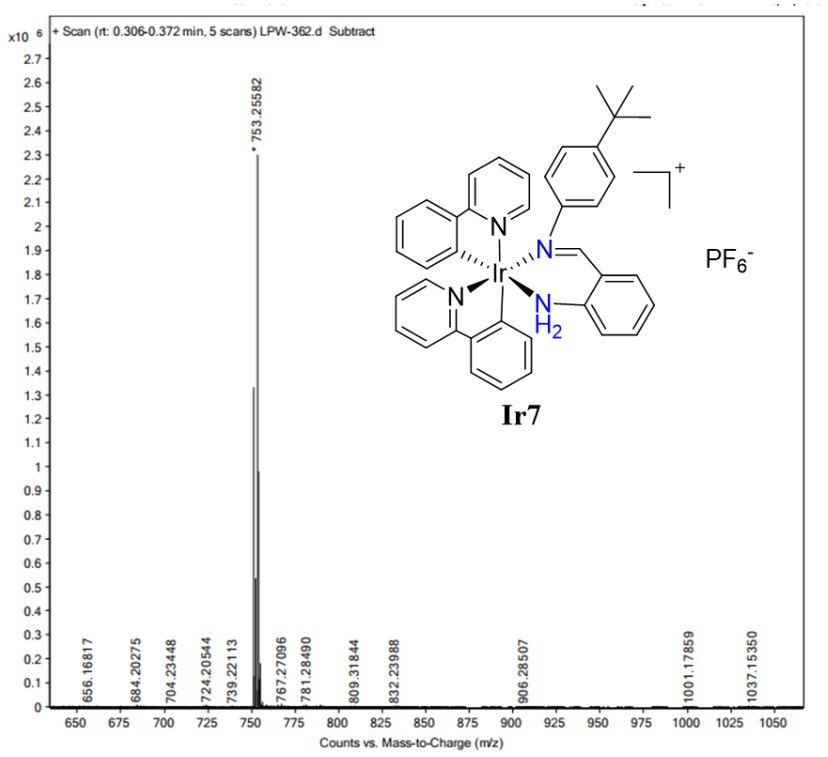

Figure S37 ESI-MS of **Ir7**.

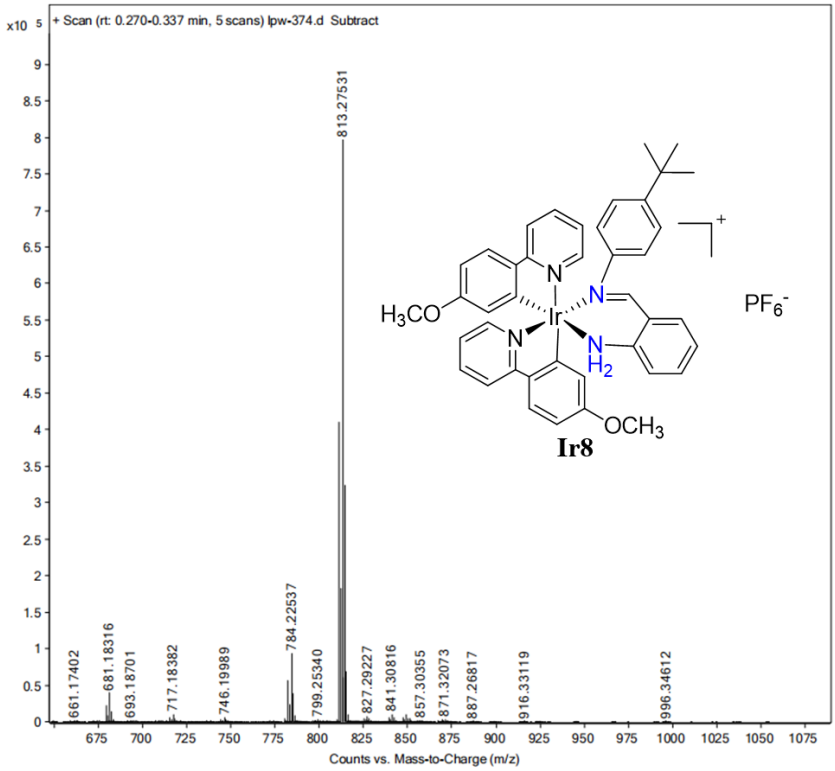

Figure S38 ESI-MS of **Ir8**.

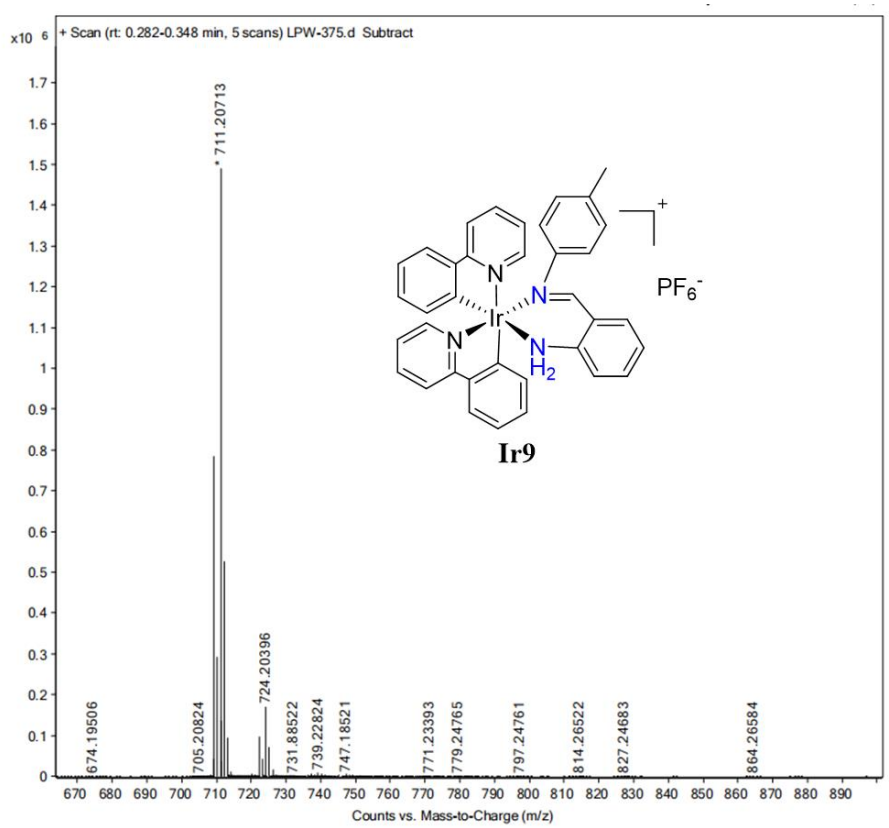

Figure S39 ESI-MS of **Ir9**.

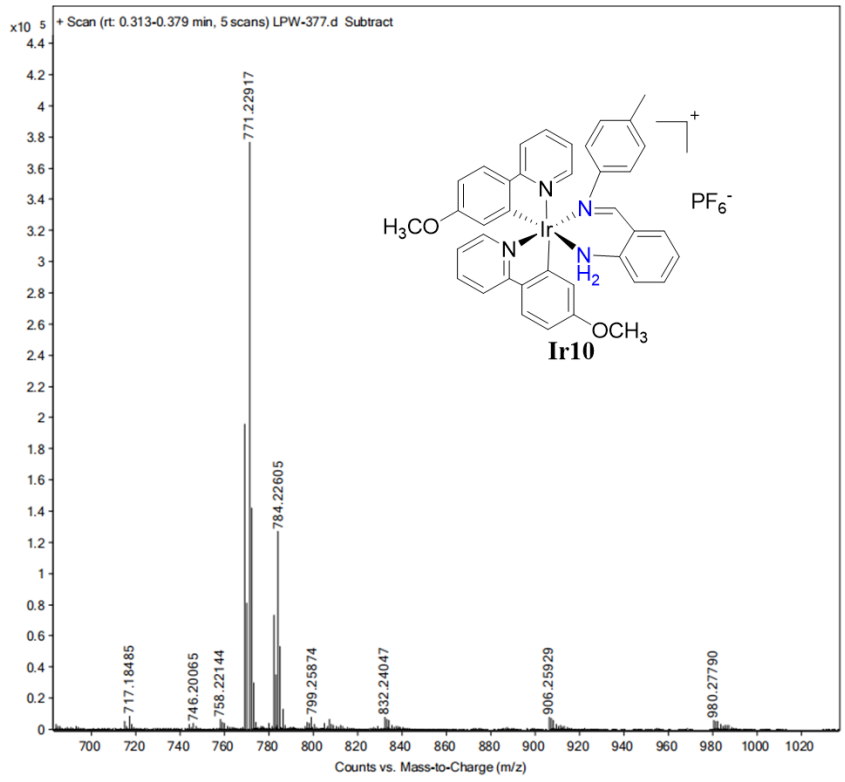

Figure S40 ESI-MS of **Ir10**

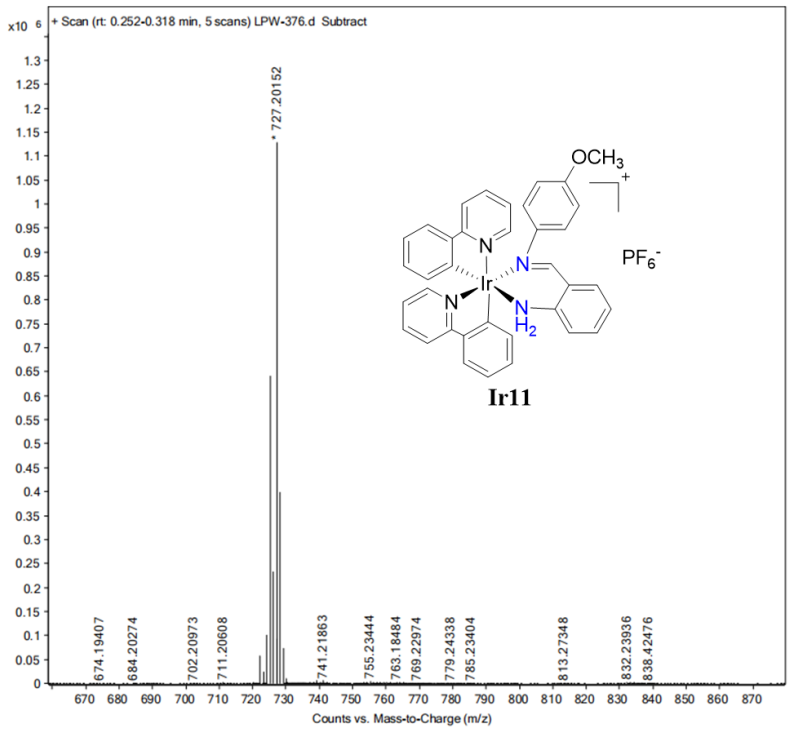

Figure S41 ESI-MS of **Ir11**.

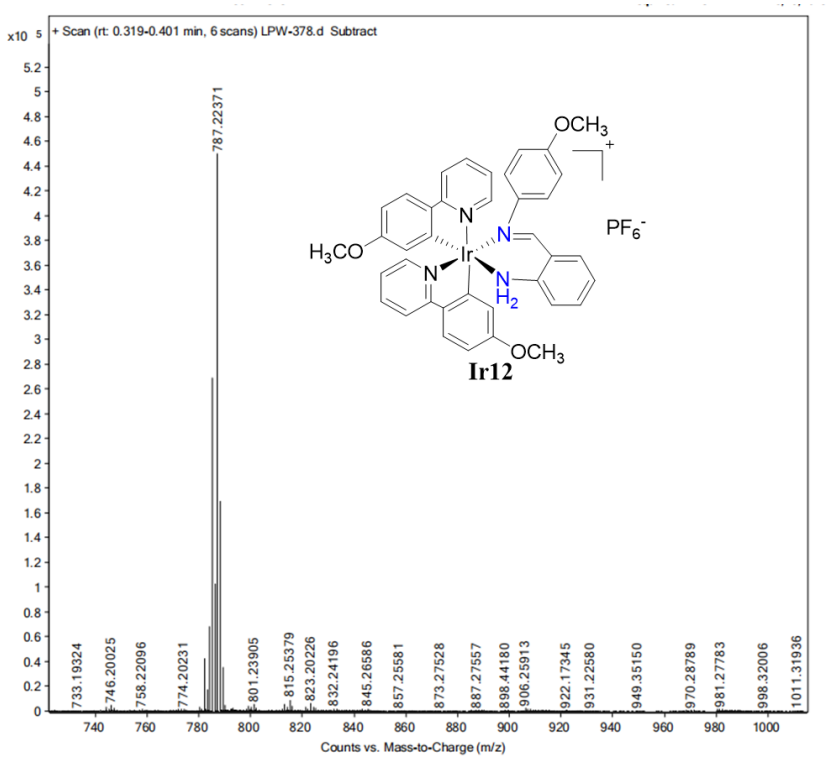

Figure S42. ESI-MS of **Ir12**.

2.3. Absorption and Emission Spectroscopy.

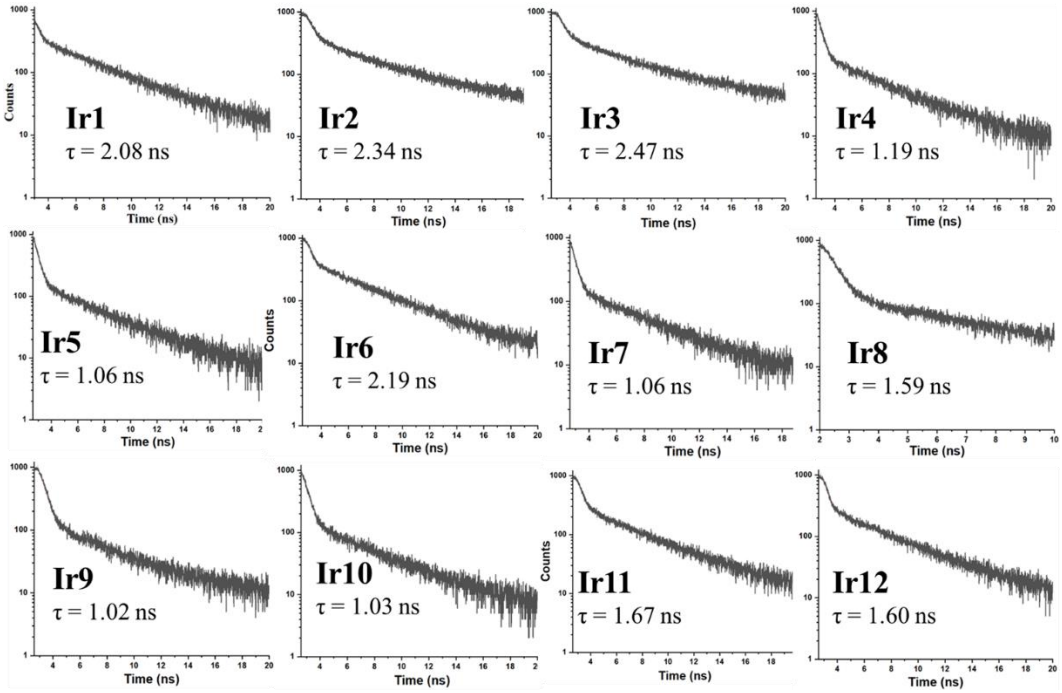

Figure S43. The average fluorescence lifetime of complexes **Ir1-Ir12**.

2.4. Reactivity and Solution Stability.

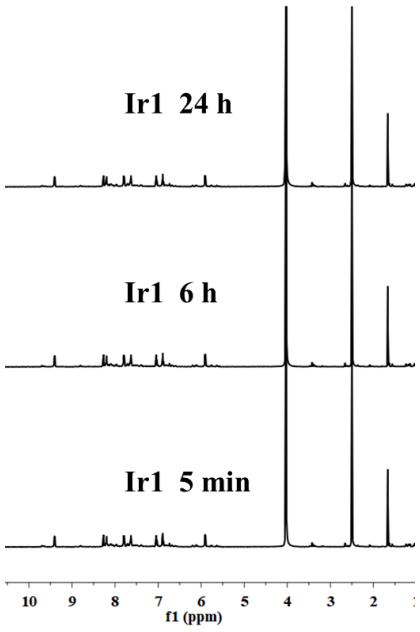

Figure S44. Time-dependent ^{1}H NMR spectroscopic stability study for **Ir1** in 75% DMSO-d_6 /25% phosphate-buffered saline (PBS) (pH ≈ 7.4, PBS is prepared from D_2O) at 37 °C after 5 min, 6 h and 24 h.

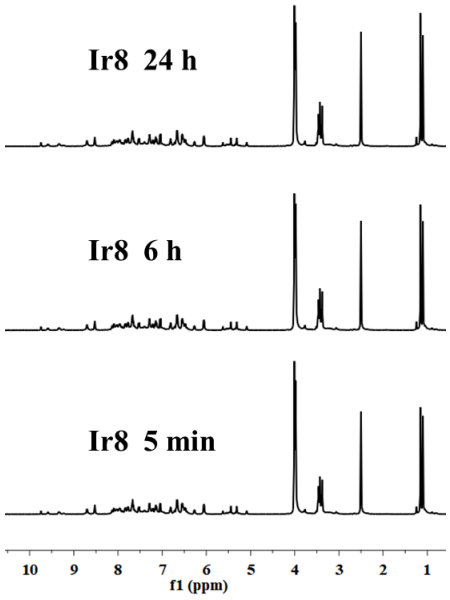

Figure S45. Time-dependent ^{1}H NMR spectroscopic stability study for **Ir8** in 75% DMSO-d_6 /25% phosphate-buffered saline (PBS) (pH ≈ 7.4, PBS is prepared from D_2O) at 37 °C after 5 min, 6 h and 24 h.

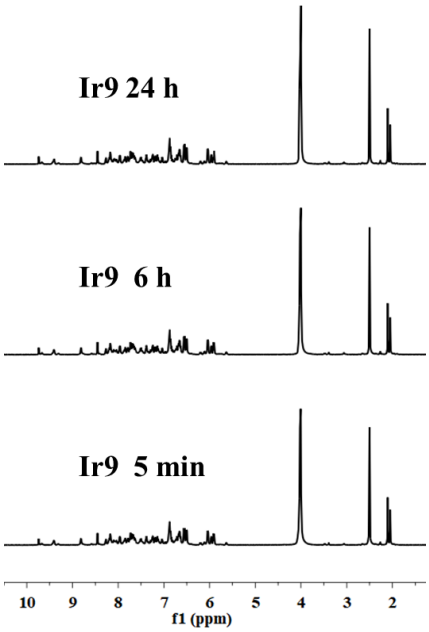

Figure S46. Time-dependent ^{1}H NMR spectroscopic stability study for **Ir9** in 75% DMSO-d_6 /25% phosphate-buffered saline (PBS) (pH ≈ 7.4, PBS is prepared from D_2O) at 37 °C after 5 min, 6 h and 24 h.

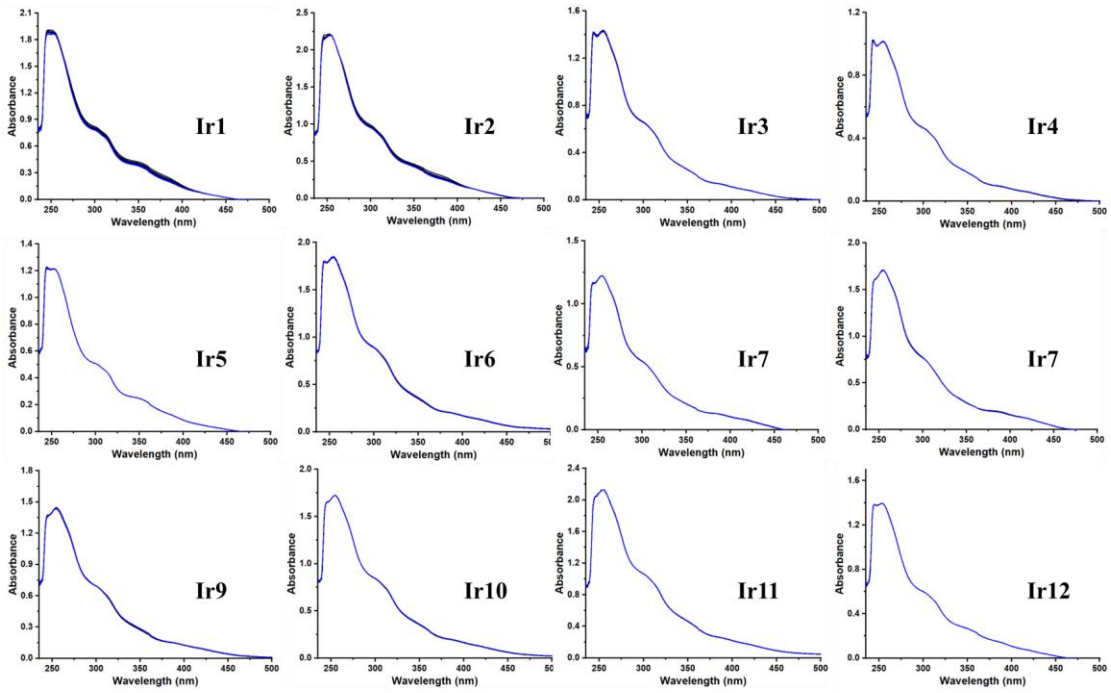

Figure S47. UV-vis spectra for complexes **Ir1-Ir12** recorded over a period of 24 h at 37°C, solution in 10% DMSO/90% PBS (v/v).

2.5. Protein Binding Studies.

The k_{sv}, K_q, K_b and n values during static quenching could be calculated using the Stern-Volmer (Equation 1) and Scatchard equation (Equation 2). The K_q of the complexes (ranging from 1.18-3.57 × 10^{13} M^{-1} s^{-1}) was about three orders of magnitude higher than that of the dynamic quenching mode (2.0 × 10^{10} M^{-1} s^{-1}), indicating that **Ir1** and **Ir7** primarily bound to BSA through the static quenching process. The binding constant (K_b) of these complexes was in a wide range from 1.26 × 10^5 to 5.01 × 10^6 (Table S6).

$$\frac{F_0}{F} = 1 + k_{SV}[Q] = 1 + K_q \tau_0 [Q] \qquad \text{(Equation 1)}$$

$$\log\left[\frac{(F_0 - F)}{F}\right] = \log K_b + n \log[Q] \qquad \text{(Equation 2)}$$

Both the reference and sample cuvettes were treated with the corresponding complexes to eliminate self-absorption. The fluorescent feature of BSA is generally

due to two protein residues called tyrosine (Tyr) and tryptophan (Trp). These residues comprise aromatic amino acids that are susceptible to alterations in their surroundings. When complexes attach to specific parts of a substance, the substance's ability to emit fluorescence is inhibited. The increase in the concentration of the complexes caused a decrease and red-shift in the absorption peak at 229 nm, which could be due to the complexes affecting the structure of the substance's alpha-helix and the polarity of its surroundings.

Synchronous fluorescence spectrometry is a method that can be used to obtain information about a fluorescent molecule at a molecular level. By maintaining a stable wavelength interval of either 15 nm or 60 nm, synchronized fluorescence can reveal the unique characteristics of Tyr or Trp residues in BSA.

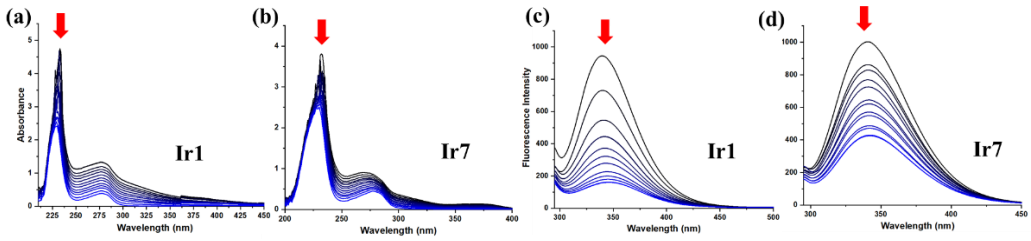

Figure S48. (a)-(b) UV-vis spectrum of BSA (10 μM) in 5 mM Tris-HCl/10 mM NaCl buffer solution (pH = 7.2) upon addition of the complexes **Ir1** and **Ir7** (0-10 μM). (c)-(d) Fluorescence spectra of BSA (10 μM; λ_{ex} = 288 nm; λ_{em} = 353 nm) in the absence and presence of the complexes **Ir1** and **Ir7** (0-10 μM). The arrow shows that the intensity changes when the concentration of the iridium(III) complex increases.

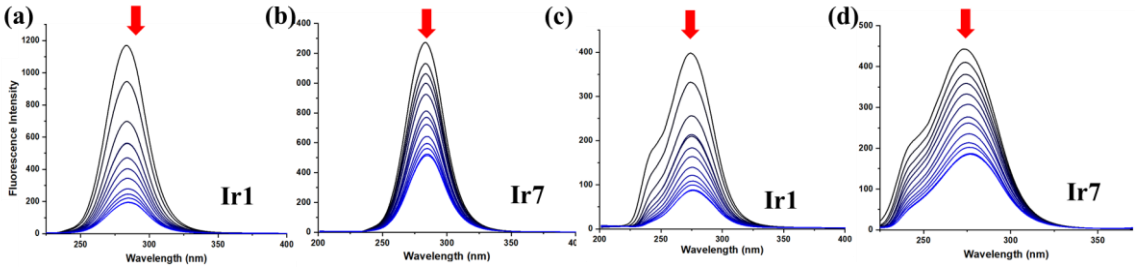

Figure S49. Fluorescence spectra of BSA with wavelength Δλ = 15 nm (a-b) and 60 nm (c-d) in the absence and presence of **Ir1** and **Ir7** (0-10 μM). The arrow shows the intensity changes when the concentration of the iridium(III) complex increases.

2.6. Cellular Uptake Pathway.

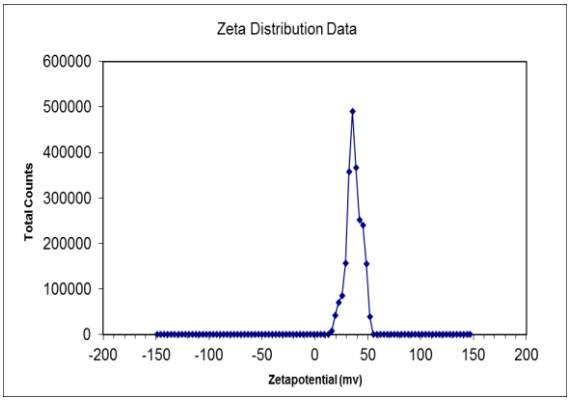

Figure S50. Zeta potential of **Ir1**.

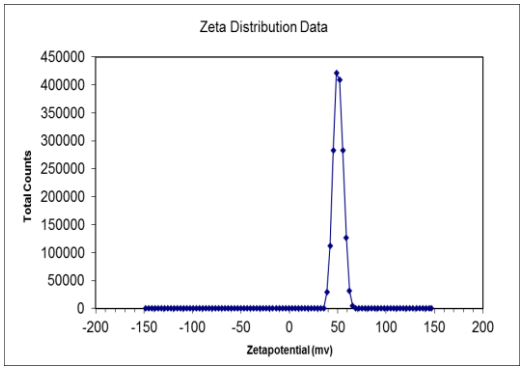

Figure S51. Zeta potential of **Ir7**.

2.7. Cellular ROS Determination.

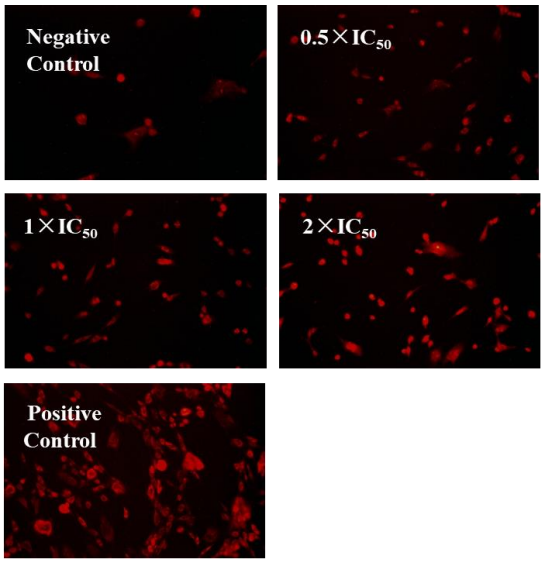

Figure S52. Analysis of ROS levels by fluorescence microscope after A549 cells were treated with **Ir1** for 24 h at 37 °C.

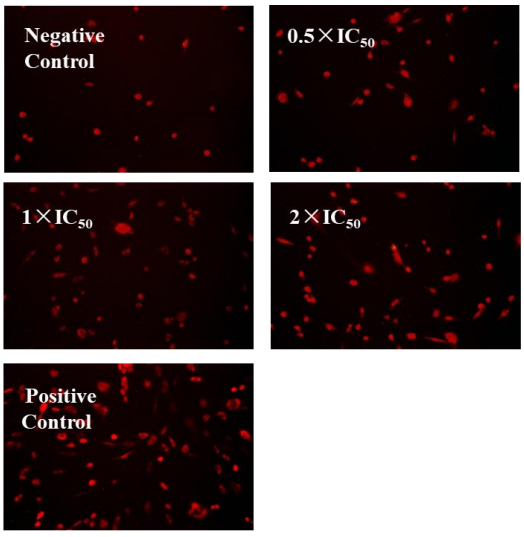

Figure S53. Analysis of ROS levels by fluorescence microscope after A549 cells were treated with **Ir7** for 24 h at 37 °C.

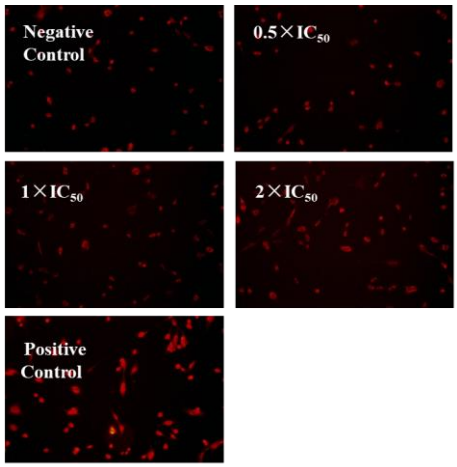

Figure S54. Analysis of ROS levels by fluorescence microscope after A549/DDP cells were treated with **Ir1** for 24 h at 37 °C.

2.8. Cell Cycle.

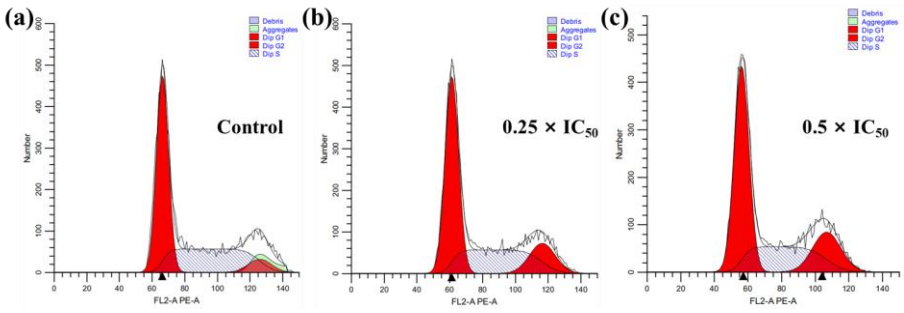

Figure S55. The cell cycle of A549 cells was analyzed by flow cytometry after induced by **Ir1** for 24 h at 37 °C, (a) Control: not treated with **Ir1**; (b) treated with 0.25 × IC_{50} of **Ir1**; (c) treated with 0.5 × IC_{50} of **Ir1**.

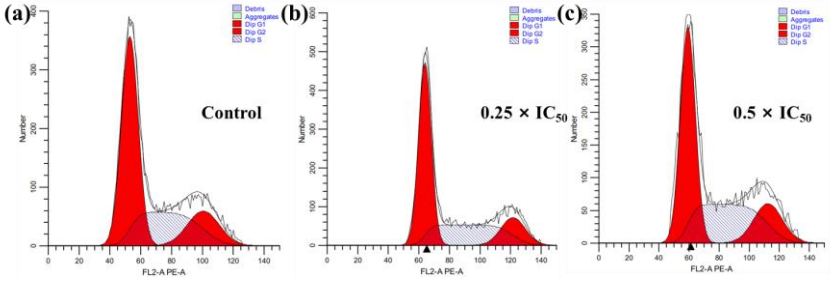

Figure S56. The cell cycle of A549 cells was analyzed by flow cytometry after induced by **Ir7** for 24 h at 37 °C, (a) Control: not treated with **Ir7**; (b) treated with 0.25 × IC_{50} of **Ir7**; (c) treated with 0.5 × IC_{50} of **Ir7**.

3. TABLES

Table S1. IC_{50} values of the ligands **L1**-**L3** and precursors **D1**-**D5** tested toward cancer cells

Ligands and Precursors	IC_{50} (μM)	
	A549	HeLa
L1	＞100	＞100
L2	＞100	＞100
L3	＞100	＞100
D1	＞100	＞100
D2	＞100	＞100
D3	＞100	＞100
D4	＞100	＞100
D5	＞100	＞100

Table S2. Flow cytometry analysis to determine the percentages of apoptotic cells, using Annexin V -FITC vs PI staining, after exposing A549 cells to complex **Ir1**

Complex	**Ir1** concentration	Population (%)			
		Viable	Early apoptosis	Late apoptosis	Non-viable
Ir1	0.25 × IC_{50}	75.3±1.6	3.29±0.06	21.3±0.6	0.13±0.02
	0.5 × IC_{50}	70.8±1.2	3.60±0.02	25.3±0.6	0.23±0.06
	1 × IC_{50}	61.5±0.9	4.08±0.07	34.2±0.2	0.30±0.03
control		94.2±2.3	0.54±0.06	4.49±0.1	0.75±0.04

Table S3. Flow cytometry analysis to determine the percentages of apoptotic cells, using Annexin V -FITC vs PI staining, after exposing A549 cells to complex **Ir7**

Complex	**Ir7** concentration	Population (%)			
		Viable	Early apoptosis	Late apoptosis	Non-viable
Ir7	0.25 × IC_{50}	2.32±0.06	0.88±0.06	80.9±1.0	15.9±0.14
	0.5 × IC_{50}	0.54±0.07	0.73±0.02	85.4±0.9	13.3±0.23
	1 × IC_{50}	1.46±0.09	0.52±0.10	86.1±1.5	11.9±0.31
control		96.6±1.5	0.52±0.03	1.25±0.11	1.64±0.05

Table S4 Flow cytometry analysis to determine the percentages of apoptotic cells, using Annexin V -FITC vs PI staining, after exposing A549/DDP cells to complex **Ir1**

Complex	**Ir1** concentration	Population (%) Viable	Early apoptosis	Late apoptosis	Non-viable
Ir1	0.25 × IC_{50}	76.5±0.6	3.18±0.08	20.2±0.1	0.21±0.04
	0.5 × IC_{50}	69.7±1.0	4.58±0.09	25.5±0.3	0.19±0.02
	1 × IC_{50}	68.3±0.9	3.92±0.3	27.6±0.1	0.17±0.01
control		94.5±1.7	0.67±0.02	4.12±0.05	0.72±0.06

Table S5. The cell cycle of A549 cells was analyzed by flow cytometry after induced by complex **Ir1** for 24 h at 37 °C

Complex	concentration	Population (%) G_0/G_1	S	G_2/M
Ir1	0.25 × IC_{50}	52.15±0.5	32.75±0.3	15.10±0.5
	0.5 × IC_{50}	52.07±0.8	28.85±0.4	19.09±0.4
control		53.32±1.0	39.99±0.8	6.69±0.2

Table S6. The cell cycle of A549 cells was analyzed by flow cytometry after induced by complex **Ir7** for 24 h at 37 °C

Complex	concentration	Population (%) G_0/G_1	S	G_2/M
Ir7	0.25 × IC_{50}	52.93±1.0	31.89±0.5	15.18±0.3
	0.5 × IC_{50}	47.49±0.9	36.08±0.3	16.43±0.2
control		53.49±1.1	29.77±0.4	16.74±0.4

Table S7. Quenching Parameters and Binding Parameters for the Interaction of **Ir1** and **Ir7** with BSA

Complexes	k_{sv} (10^5 M^{-1})	K_q (10^{13} M^{-1} S^{-1})	K_b (10^5 M^{-1})	n
Ir1	3.57±0.14	3.57	50.11	1.42
Ir7	1.18±0.08	1.18	1.26	1.22